



What does Seismic Anisotropy tell us about the Lithosphere-Asthenosphere Boundary?

Jean-Paul Montagner⁽¹⁾,

Gael Burgos ⁽¹⁾, Eric Beucler ⁽²⁾, Antoine
Mocquet⁽²⁾ and Yann Capdeville⁽²⁾, Mathias
Obrebski^(1,3), Lev Vinnik⁽⁴⁾.....

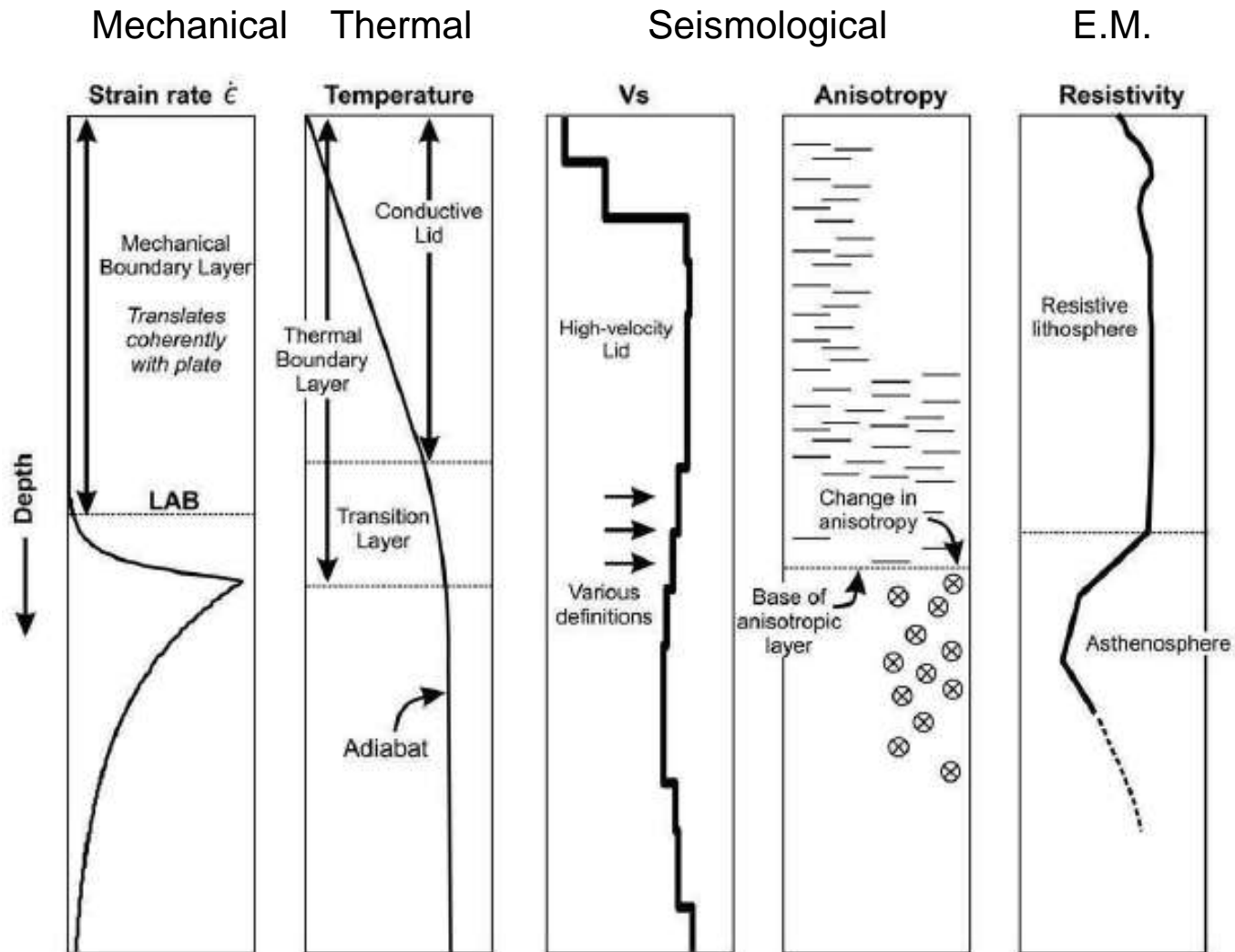
1- Laboratoire Sismologie, I.P.G., Paris, France

2- L.P.G., University of Nantes, Nantes, France

3- LDEO, New-York, U.S.A.

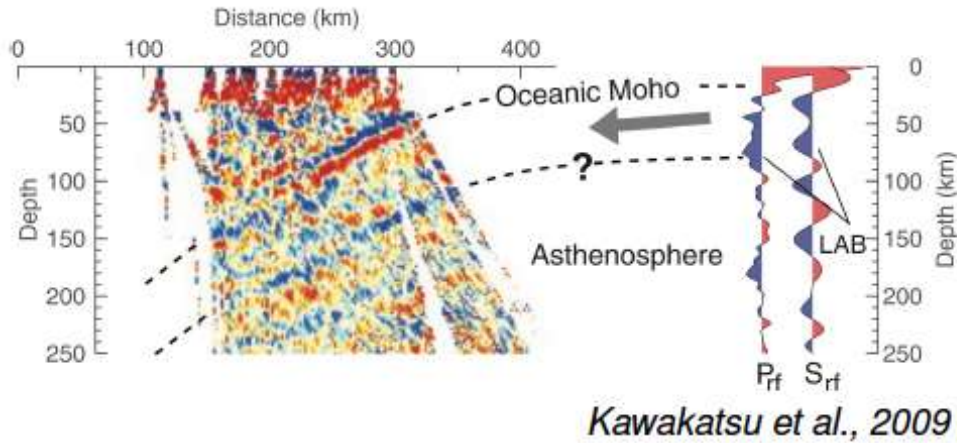
4- I.P.E., Moscow, Russia

L.A.B.: Lithosphere-Asthenosphere Boundary (many different approaches and definitions)

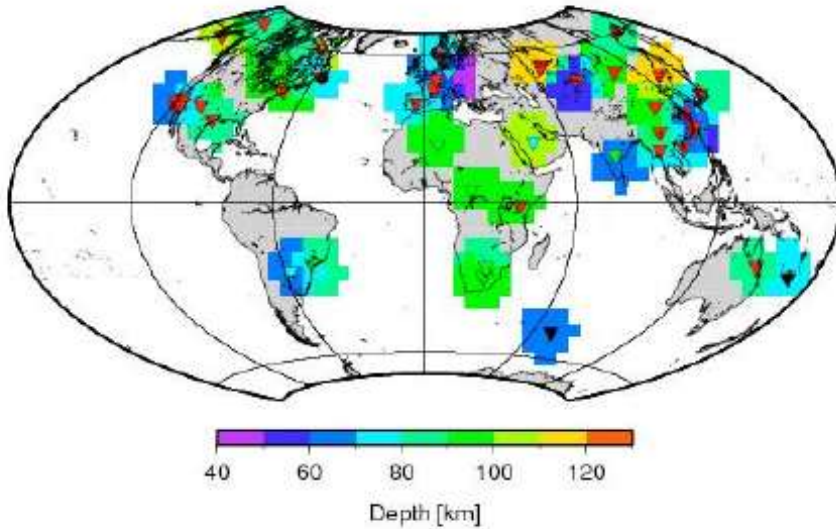
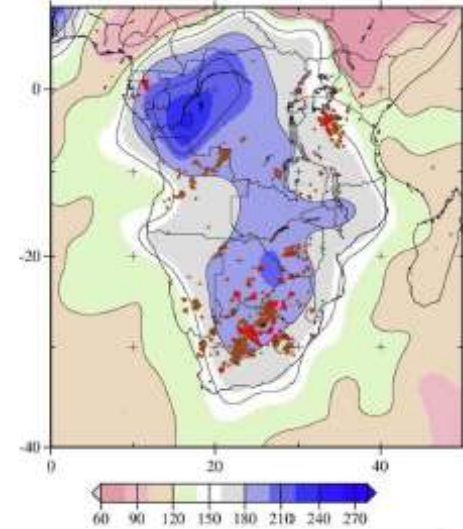


LAB : from seismic data

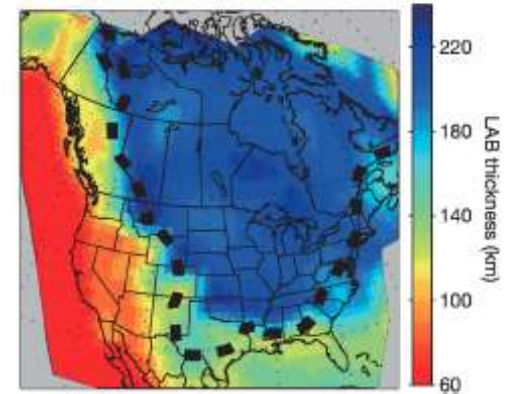
Receiver functions



Surface waves



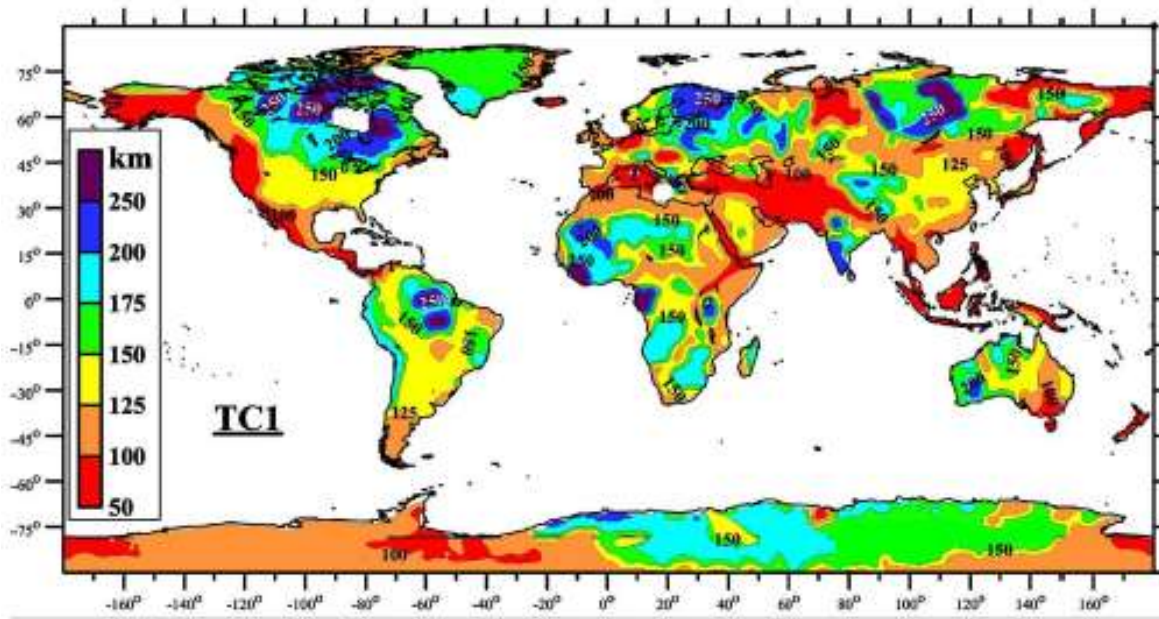
Fishwick, 2010



+SKS

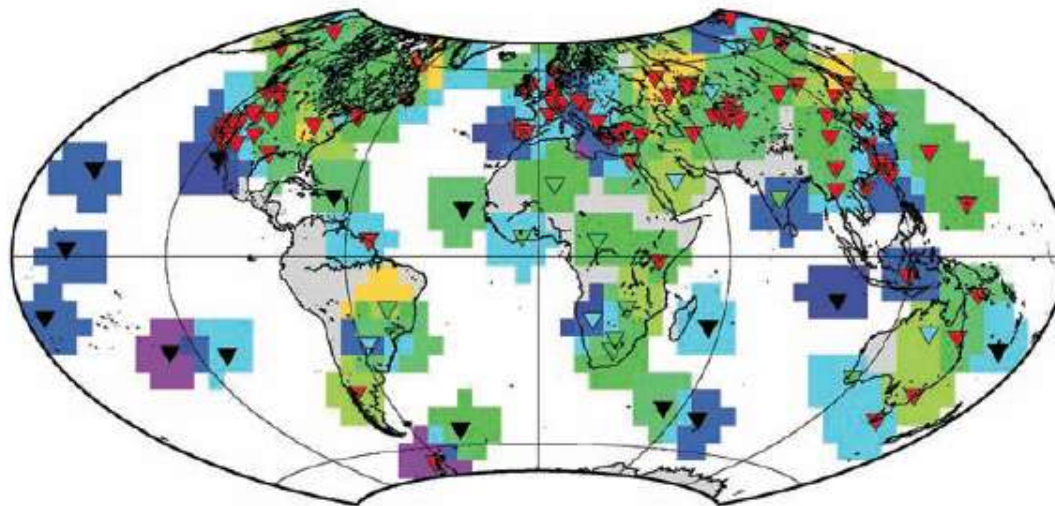
Yuan & Romanowicz, 2010

Rychert & Shearer, 2009



Global scale

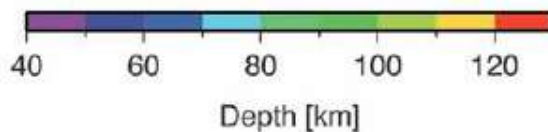
Artemieva, 2006



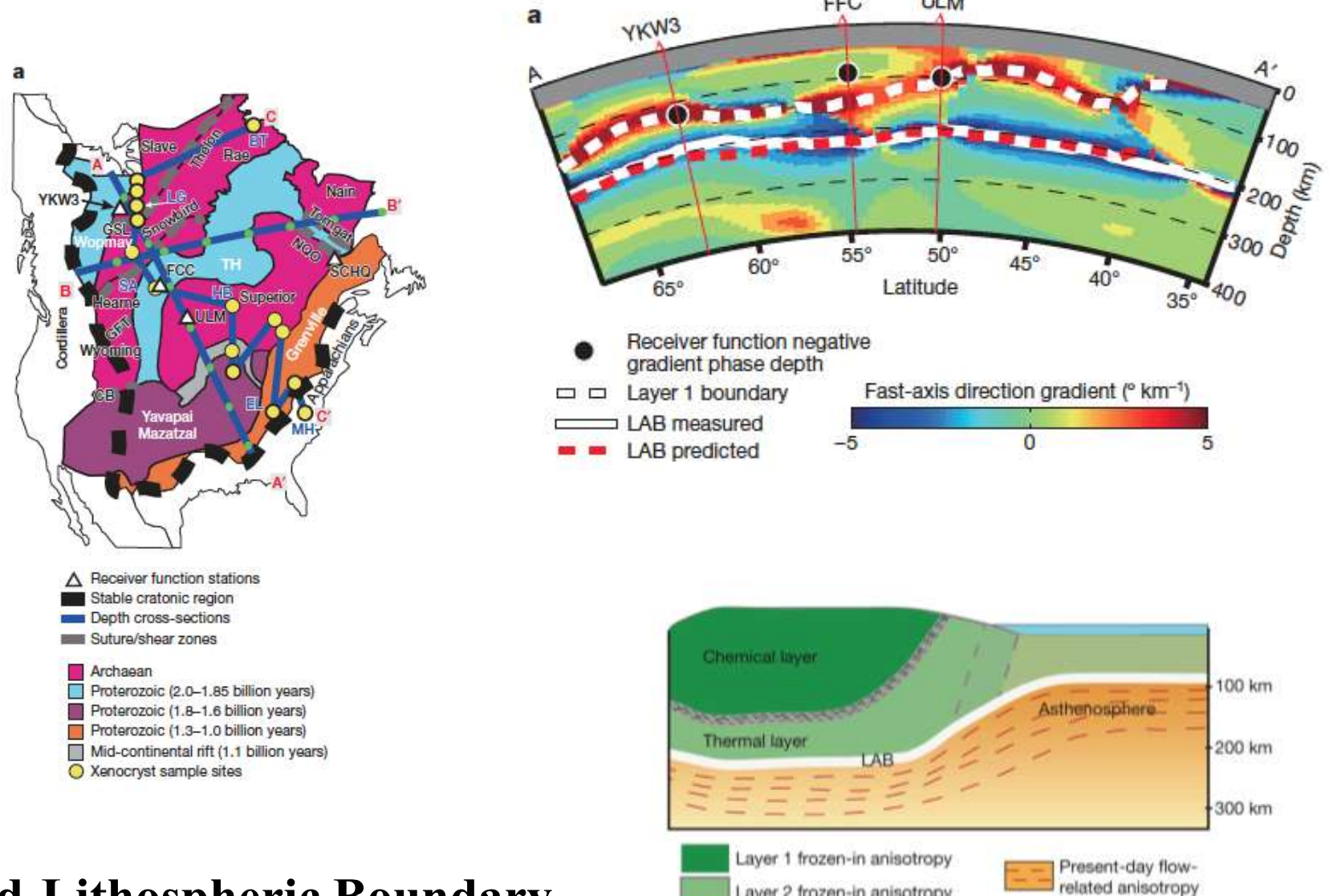
- Much discrepancy Between different Estimates
- Global tomographies give 200-250km depth for continental roots

-Ocean-Continent

Rychert et al., 2009



Structure of continents from seismic anisotropy

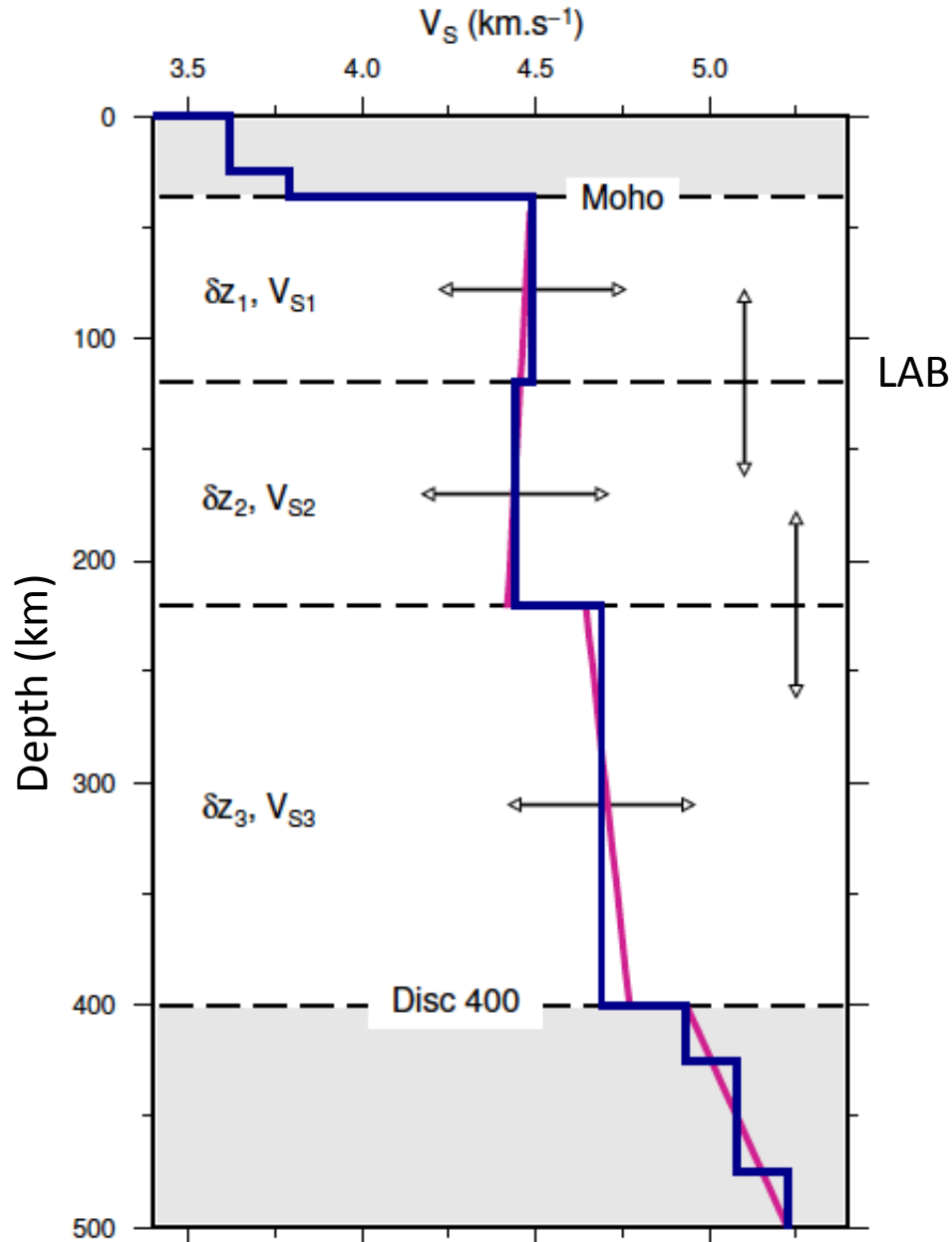


Mid-Lithospheric Boundary

Yuan and Romanowicz, 2010

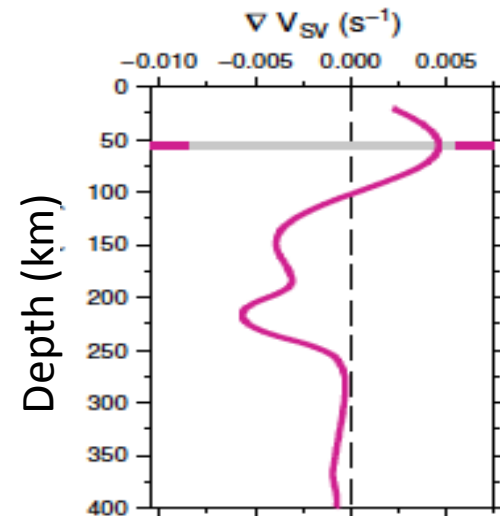
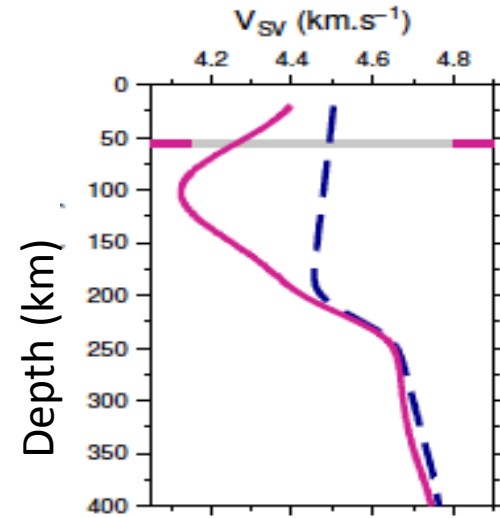
From Surface wave dispersion

Statistical Monte-Carlo Approach



First order Perturbation theory
(from phase velocity inversion)

Proxy from parameter V_{SV}



Proxies from other parameters: Seismic Anisotropy?

Well resolved parameters:

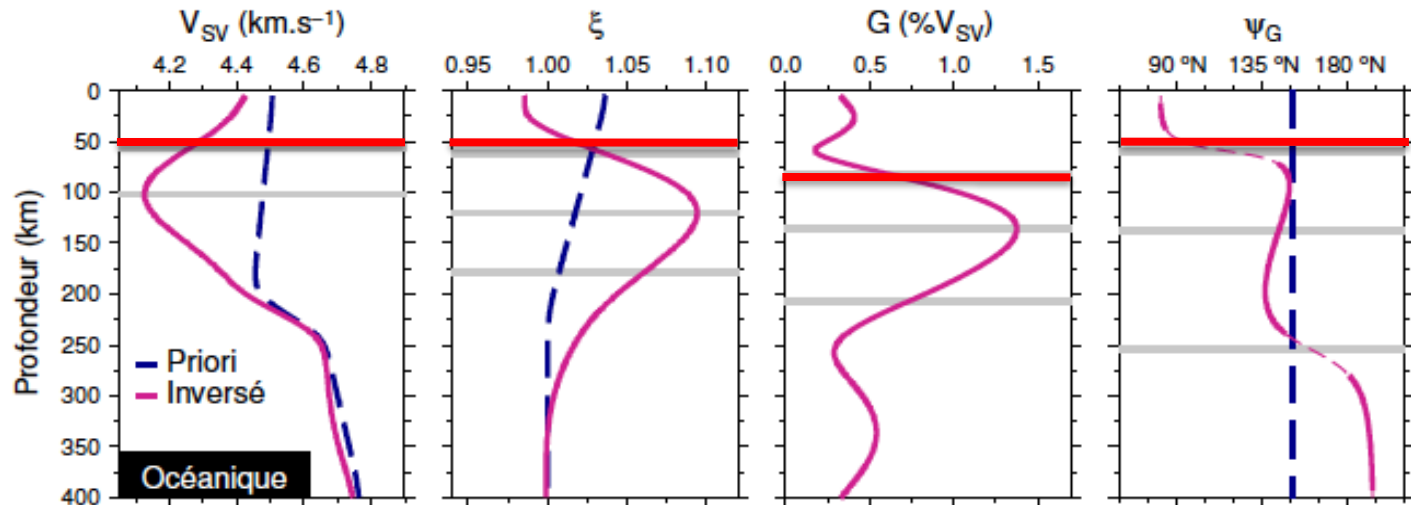
V_{SV} S-wave velocity

ξ , radial anisotropy

G, Ψ_G S-wave azimuthal anisotropy

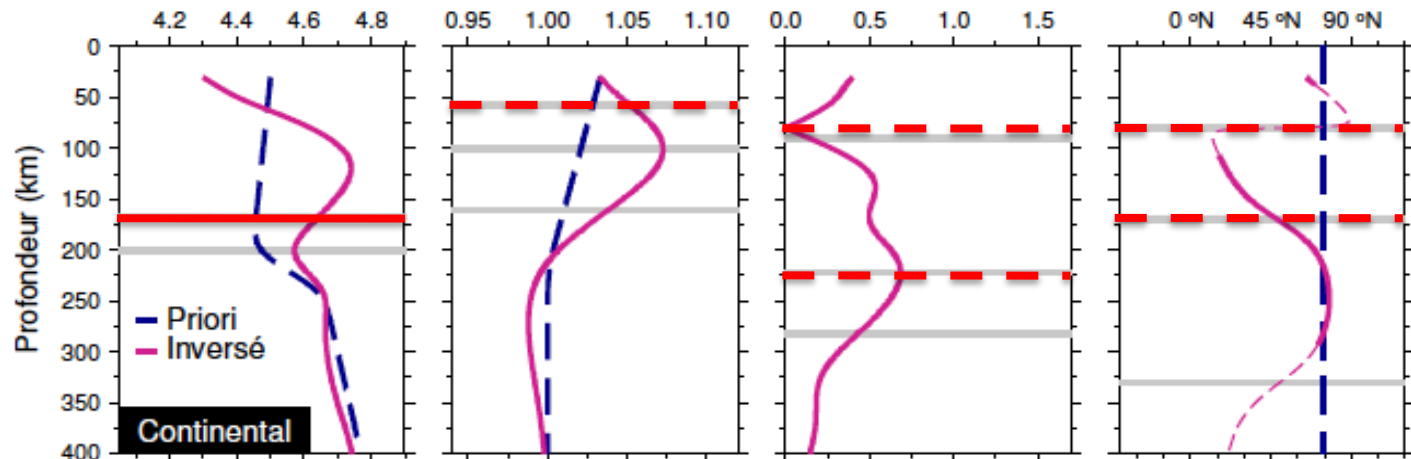
Oceanic profile

$\lambda=35^\circ, \phi=-35^\circ$



Continental profile

$\lambda=63^\circ, \phi=-96^\circ$





Seismic Anisotropy at all scales

-From microscopic scale up to macroscopic scale

-Efficient mechanisms of alignment of minerals in the crust and upper mantle:

(L.P.O.: Lattice preferred orientation of minerals;

S.P.O.: Shape preferred orientation: fluid inclusions, cracks...

Fine Layering)

ANISOTROPY is the Rule not the Exception

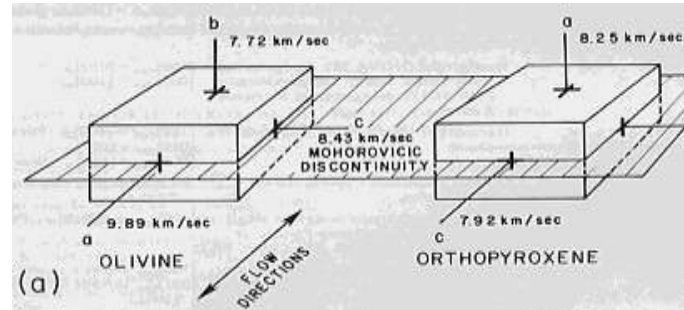
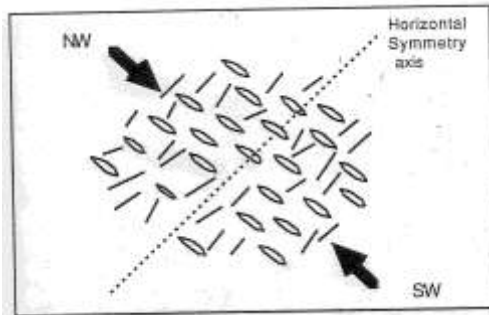
Apparent (observed) anisotropy:

NON UNIQUE INTERPRETATION

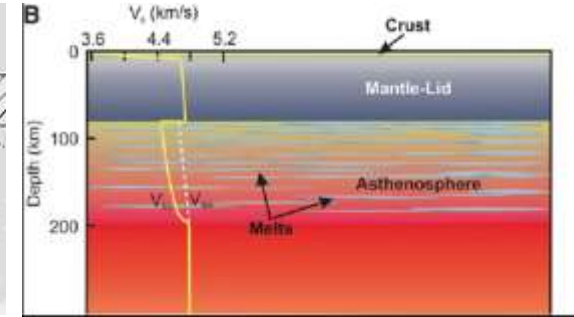
in different depth ranges of the Earth

Different processes in different layers

-S.P.O. (stress) -L.P.O.(strain) Fine Layering



Christensen and Lundquist (1982)



Kawakatsu et al. (2009)

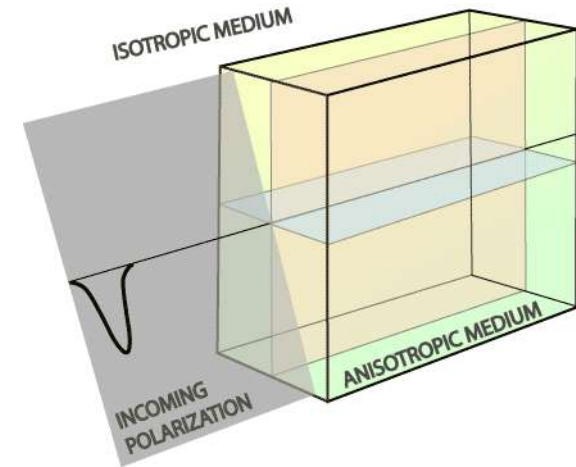
- **Mineralogy, Water and fluid content**
- **Present day tectonic, geodynamic processes**
- **Past processes (frozen anisotropy)**

**Separation of the different kinds of anisotropy
in different layers => Different interpretations**

**Stratification of anisotropy in the crust & mantle
Above, below the LAB?**



Different kinds of anisotropy effects on seismic waves



- Body waves: Shear wave splitting (birefringence)
- Surface waves (Rayleigh and Love):
 - Rayleigh-Love discrepancy (VTI model: radial anisotropy)
 - Azimuthal variations of phase or group velocities
 - Amplitude effects: Quasi-Rayleigh, Quasi-Love polarization anomalies

Courtesy of Ed. Garnero

Effect of anisotropy on the phase of surface waves

Effect on eigenfrequency ω_k (Rayleigh's principle)

$$\frac{\Delta\omega_k}{\omega_k} = \frac{\int_{\Omega} \varepsilon_{ij}^* \delta C_{ijkl} \varepsilon_{kl} d\Omega}{\int_{\Omega} \rho_0 u_r^* u_r d\Omega} = \frac{\delta V}{V} \Big|_k$$

ε strain tensor, u displacement, δC_{ijkl} elastic tensor perturbation (21 elastic moduli), V phase velocity

Phase velocity perturbation $\delta V(T, \theta, \phi, \Psi)$ at point $r(\theta, \phi)$
(Smith & Dahlen, 1973; Montagner & Nataf, 1986)

Ψ Azimuth (angle between North and wave vector)

$$\delta V(T, \theta, \phi, \Psi) / V = \alpha_0(T, \theta, \phi) + \alpha_1(T, \theta, \phi) \cos 2\Psi + \alpha_2(T, \theta, \phi) \sin 2\Psi + \alpha_3(T, \theta, \phi) \cos 4\Psi + \alpha_4(T, \theta, \phi) \sin 4\Psi$$

• *Cijkl 21 elastic moduli*

□ $\alpha_0 = 0$ - ψ term: 5 parameters A, C, F, L, N (PREM)

VTI Model (transverse isotropy with vertical symmetry axis)

• *Best resolved parameters from surface waves (among 13 parameters when including azimuthal anisotropy 2ψ -, 4ψ - terms)*

$$L = \rho V_{SV}^2 \quad \text{Isotropic part of } V_{SV}$$

$$N/L = \xi = (V_{SH}/V_{SV})^2 \quad \text{Radial Anisotropy}$$

G, Ψ_G Azimuthal Anisotropy of V_{SV} , also related to SKS splitting (when horizontal symmetry axis, vertical propagation, Montagner et al., 2000)

• *Body waves (Crampin, 1984)*

$$\rho V_{SV}^2 = L - G_c \cos 2\Psi + G_s \sin 2\Psi$$

$$\rho V_{SH}^2 = N - E_c \cos 4\Psi - E_s \sin 4\Psi$$

Proxies from other parameters: Seismic Anisotropy

Well resolved parameters:

V_{SV} S-wave velocity

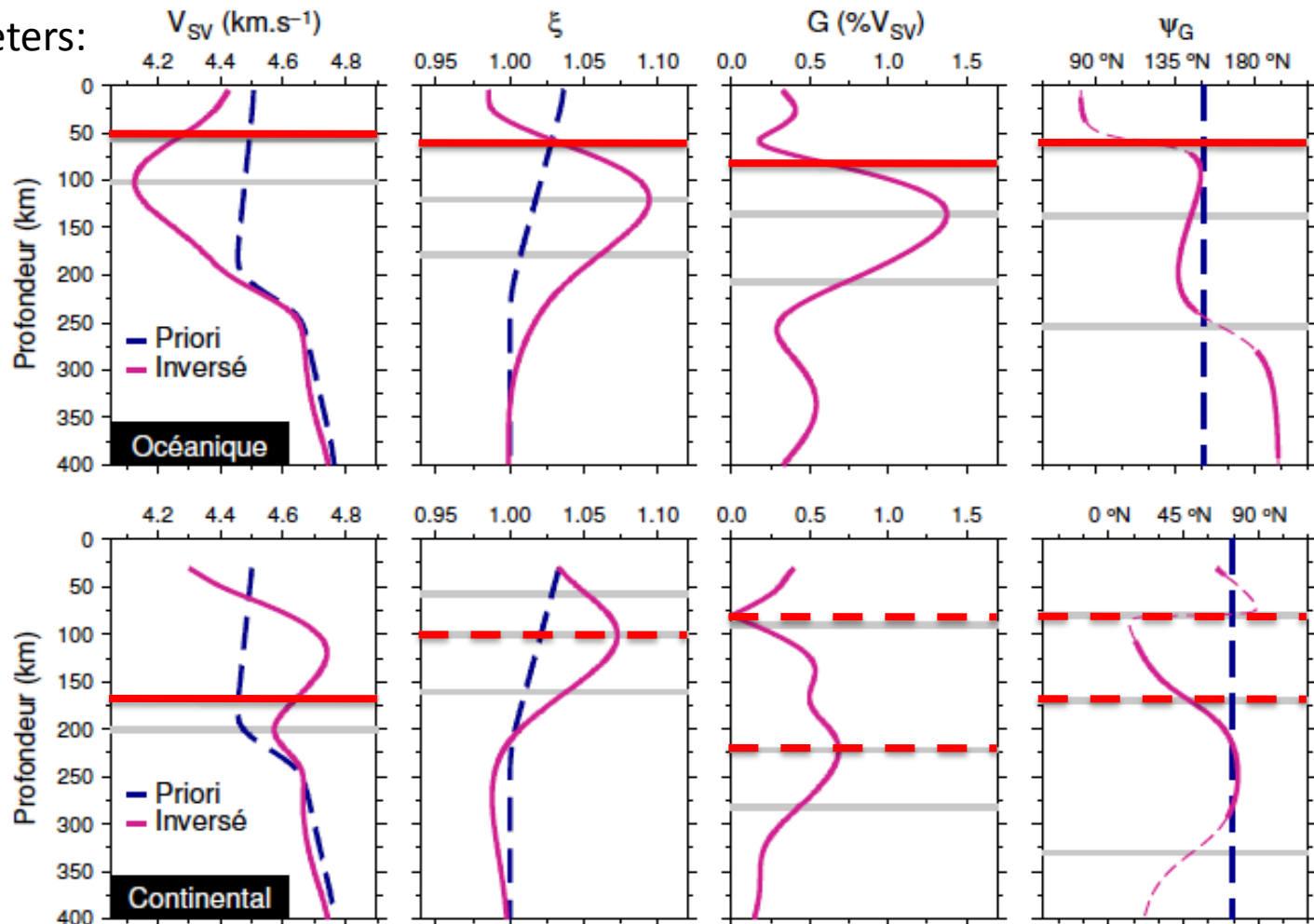
ξ , radial anisotropy

G , Ψ_G S-wave

azimuthal anisotropy

Oceanic profile

$\lambda=35^\circ$, $\phi=-35^\circ$



Continental profile

$\lambda=63^\circ$, $\phi=-96^\circ$

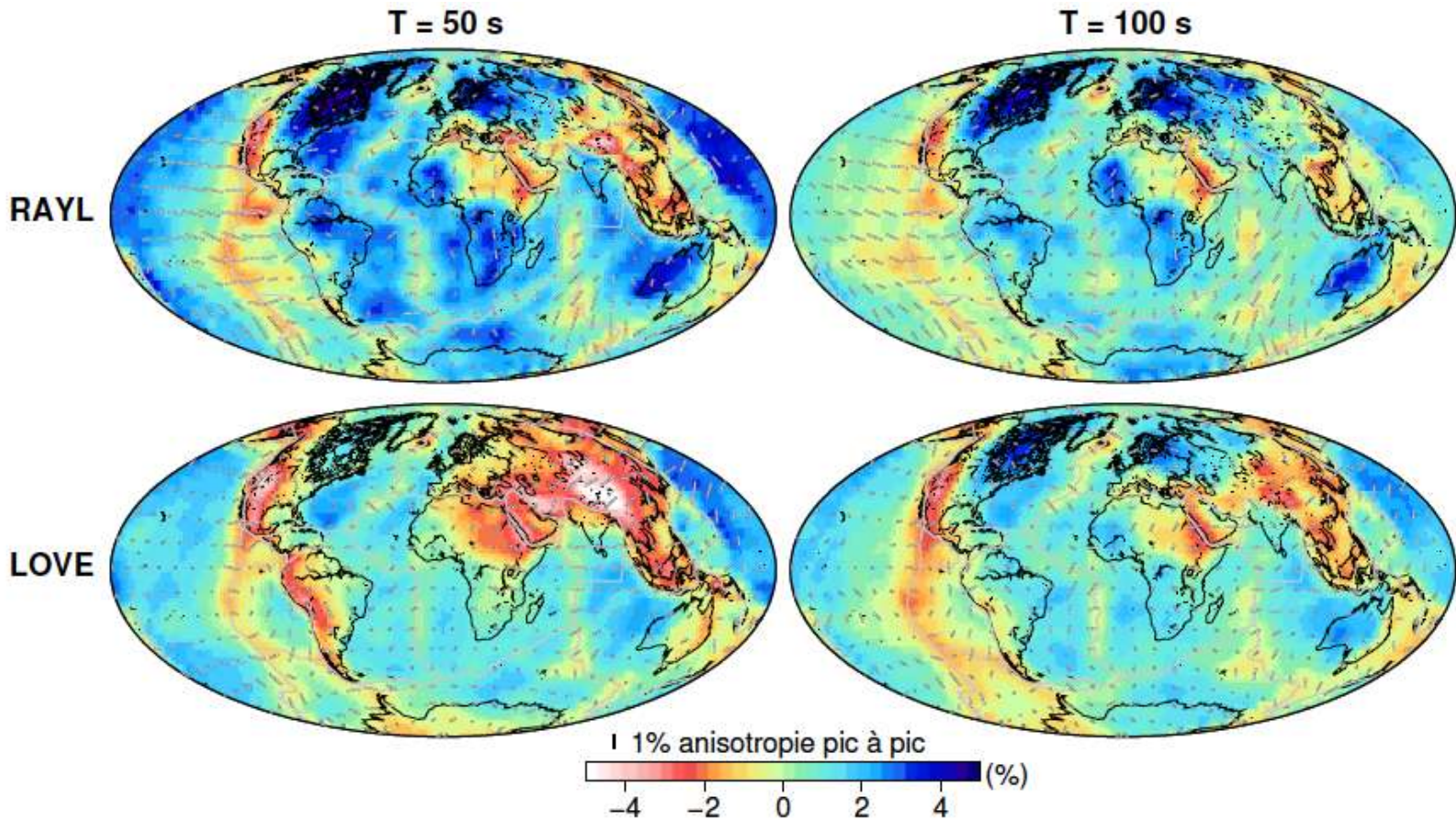
Data collection

Phase and group velocity dispersion curves
Rayleigh and Love waves,
Fundamental and higher modes ($n=\{0,6\}$)

IPGP(1)	44 - 315	9292†	-	-
UTRECHT(2)	35 - 175	63628	35 - 176	45179
HARVARD(3)	35 - 150	37738	35 - 150	23227
BOULDER(4)	16 - 200	76580	16 - 150	47021
TOTAL	-	187238	-	115427

First step: Regionalization => local dispersion velocity $V(T, \theta, \phi, \psi)$

Rayleigh phase velocity and azimuthal anisotropy



Second step: Inversion at depth

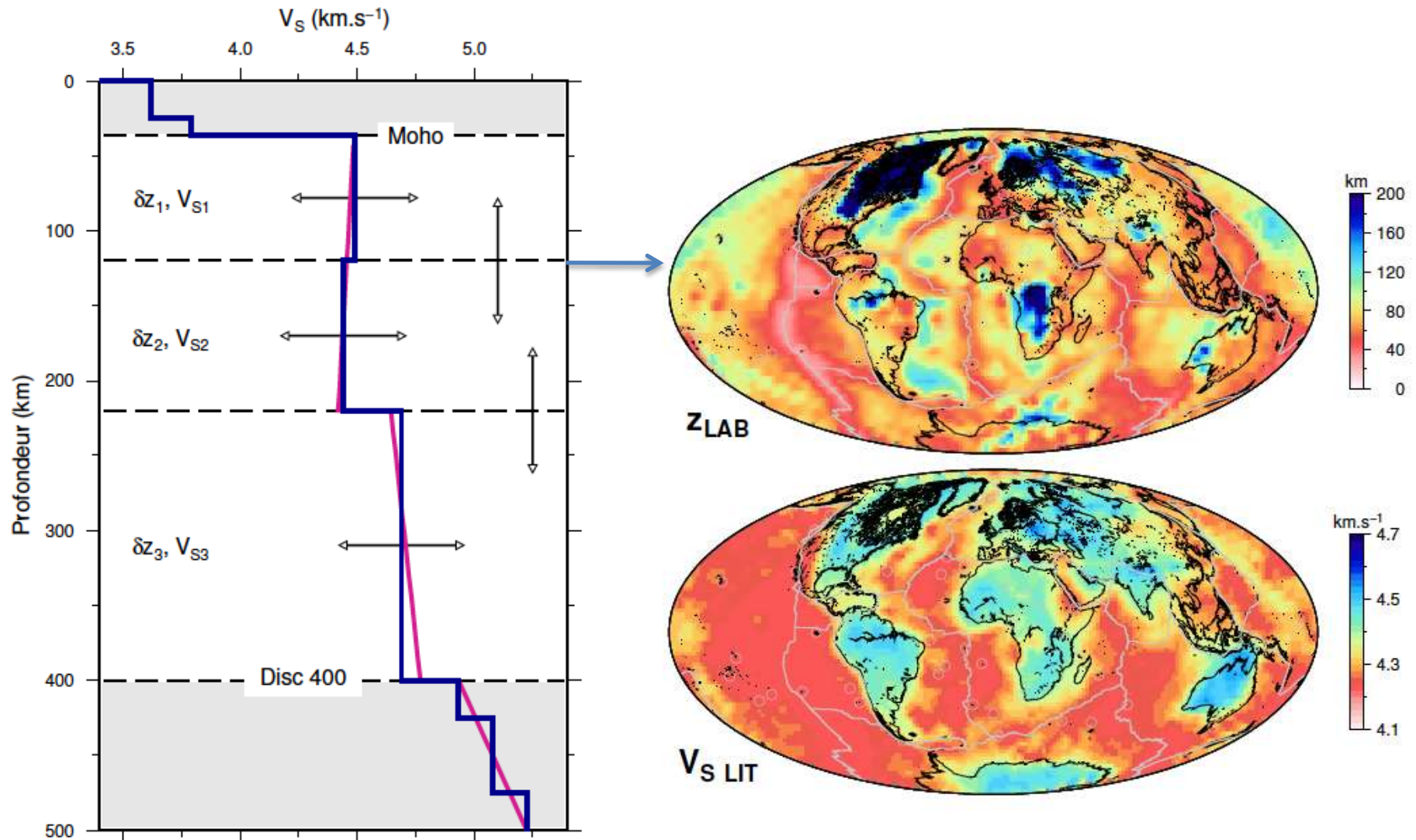


Statistical Monte-Carlo Inversion

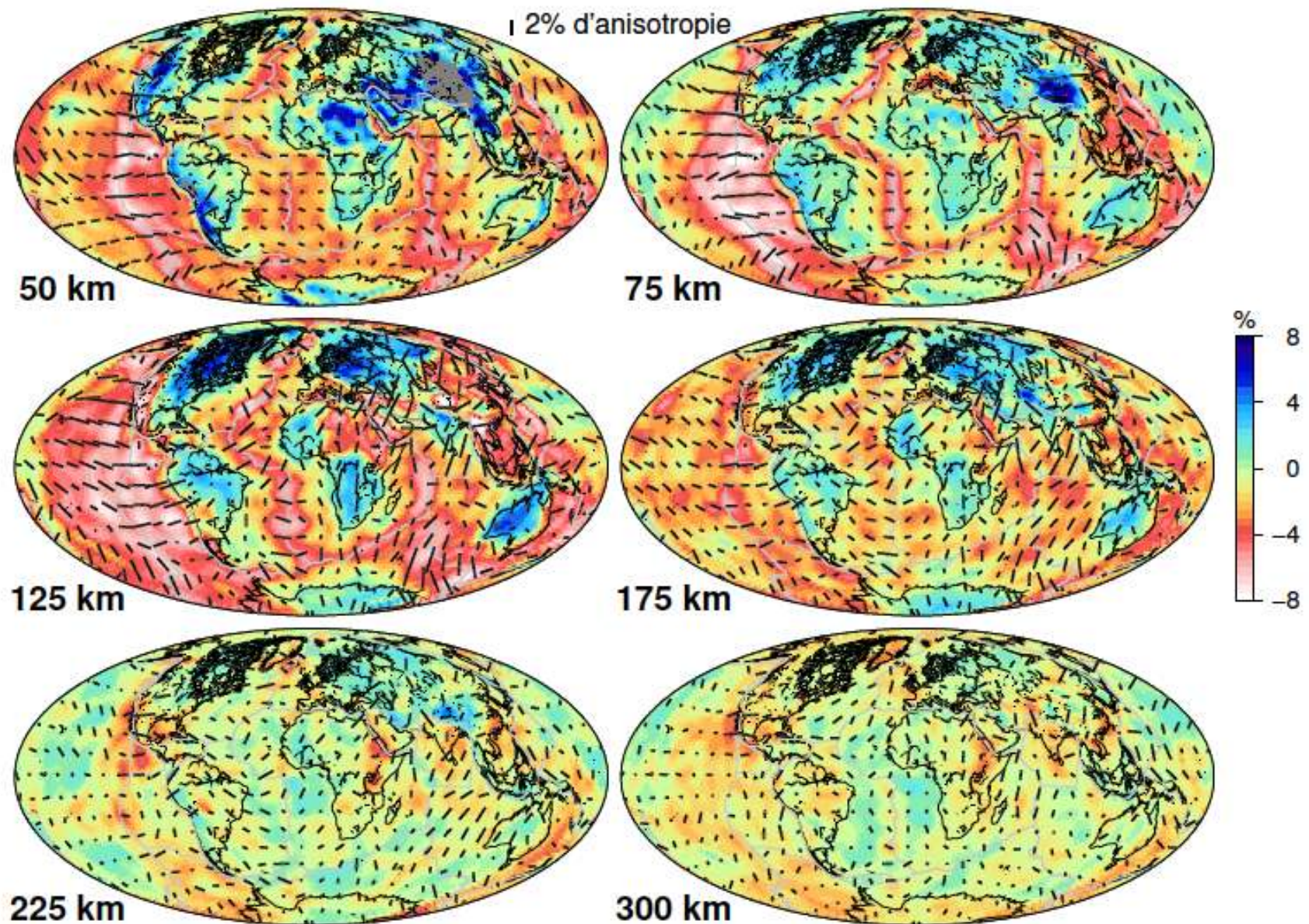
First order Perturbation

LAB: Statistical M.C. Inversion

Data: C_R , C_L , U_R , U_L [30-300s], Parameters: 3Vs, 2 δz



First order perturbation Theory => depth distribution of V_{sv} , G (and ξ)



Proxies obtained from anisotropic tomographic models

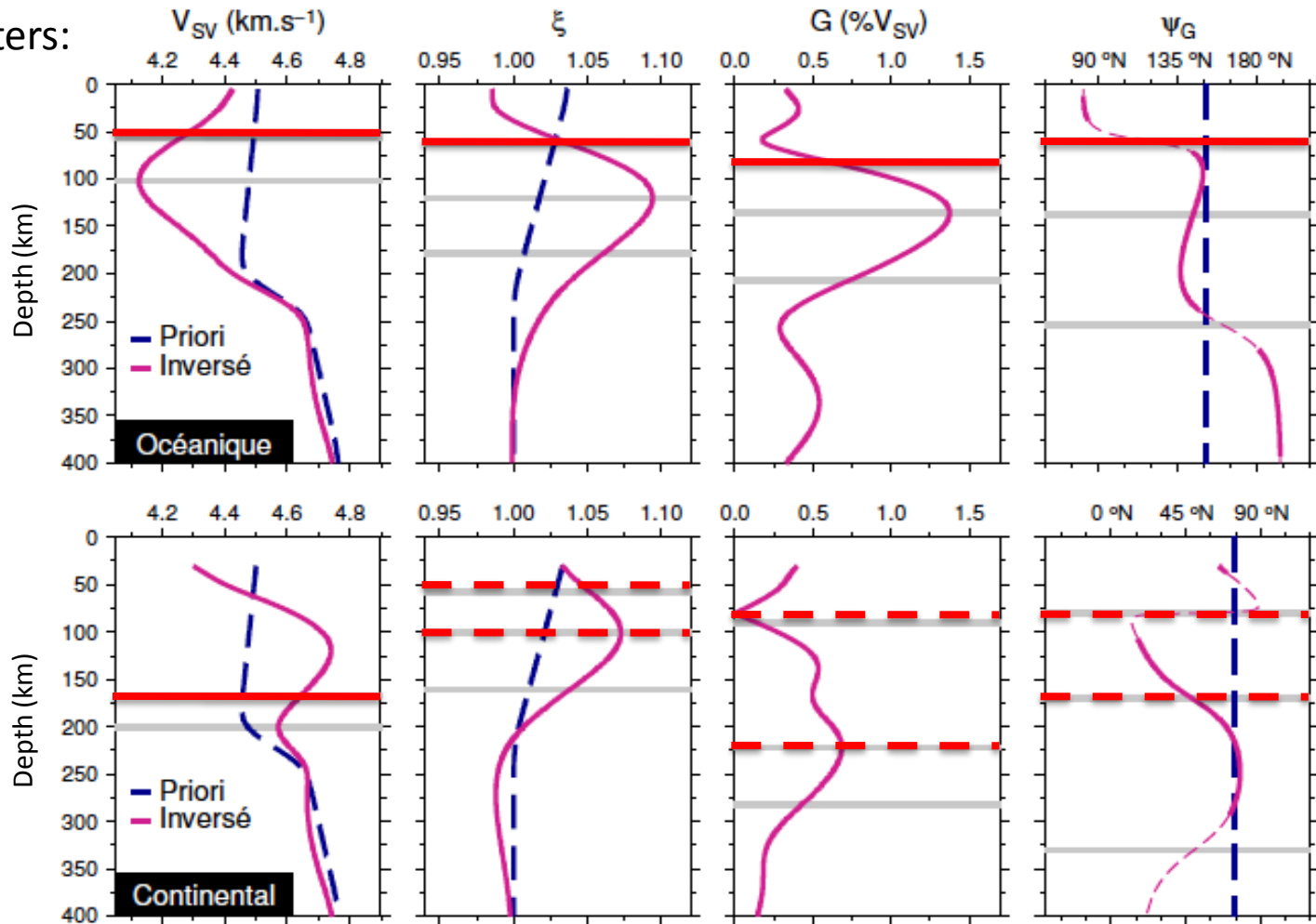
Well resolved parameters:

V_{SV} S-wave velocity

ξ , radial anisotropy

G , Ψ_G S-wave

azimuthal anisotropy



Oceanic profile

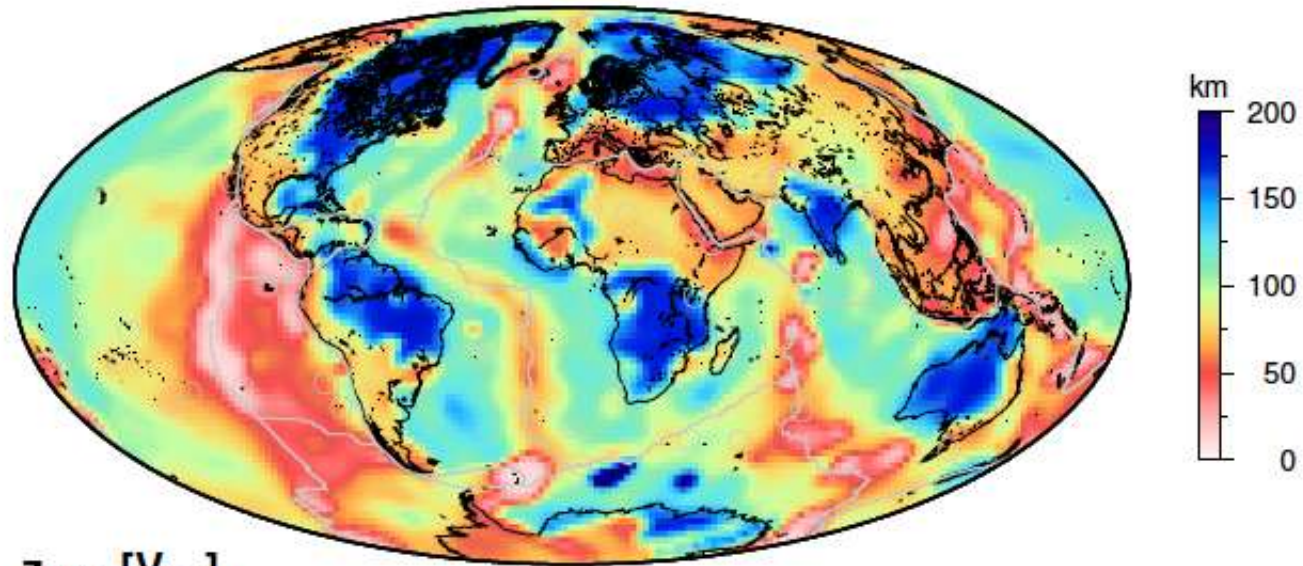
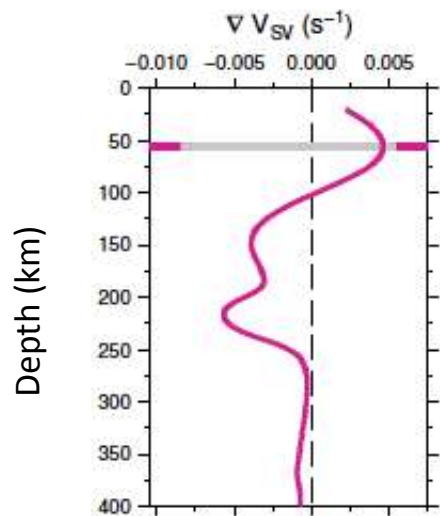
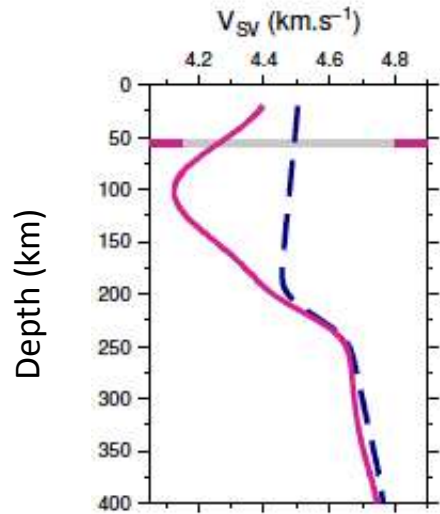
$\lambda=35^\circ$, $\phi=-35^\circ$

Continental profile

$\lambda=63^\circ$, $\phi=-96^\circ$



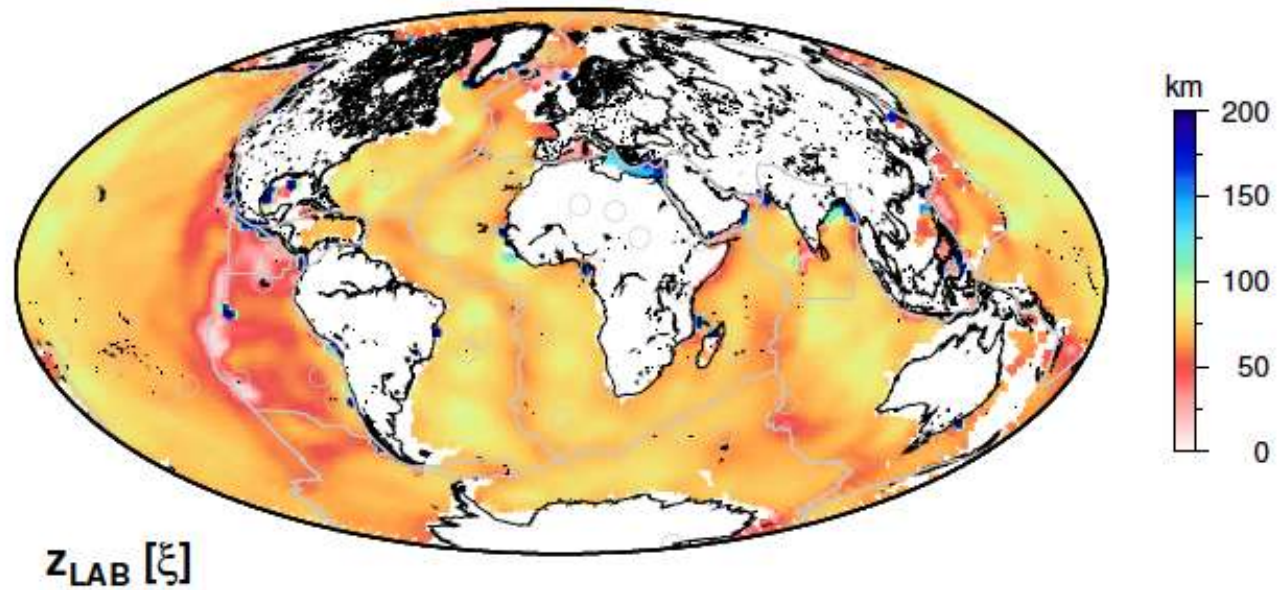
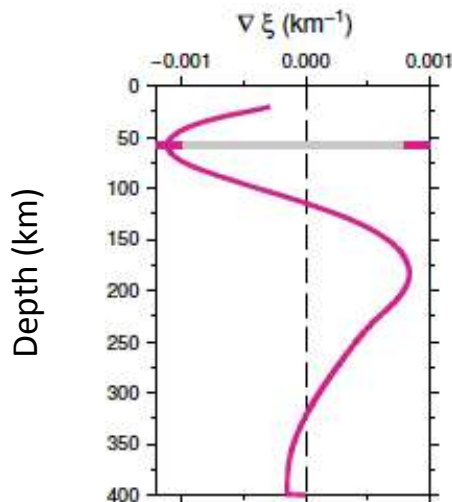
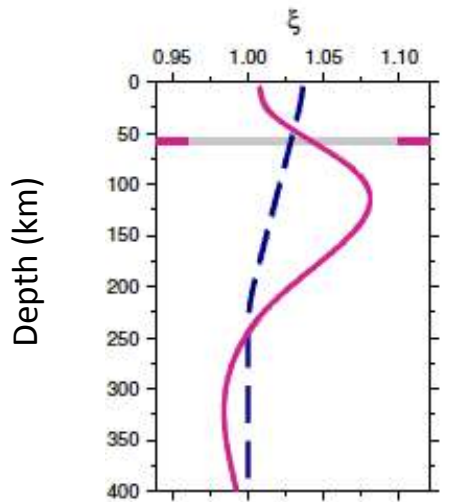
LAB from the gradient of VSV parameter



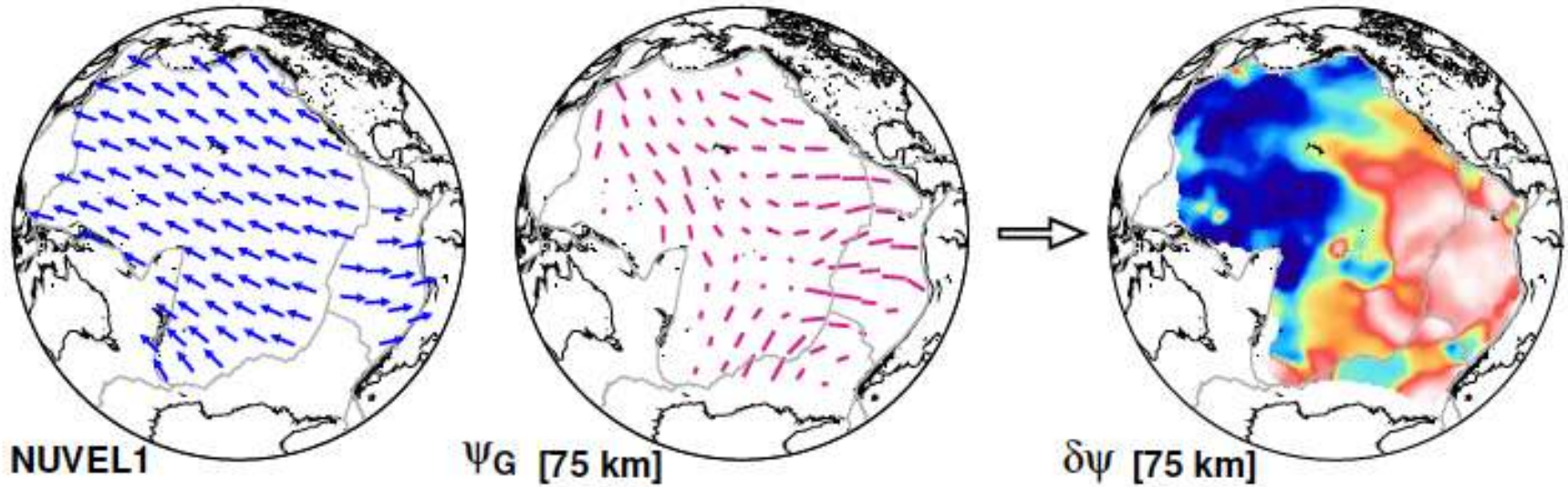
z_{LAB} [V_{SV}]

LAB from the gradient of ξ parameter (only oceans)

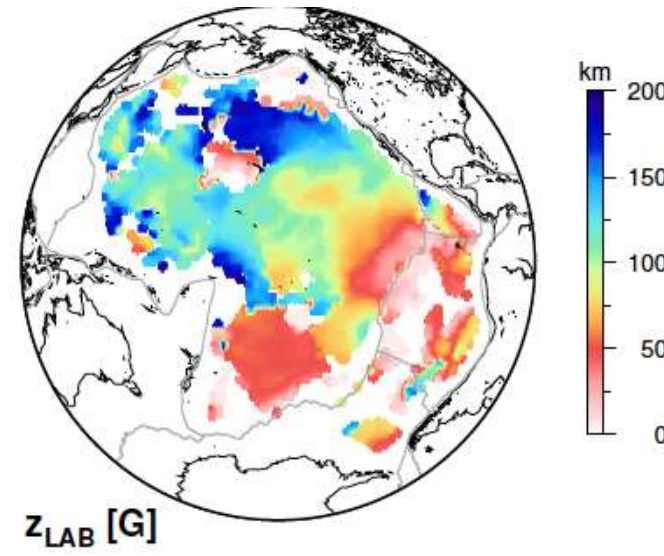
$$\text{Radial anisotropy } \xi = (V_{SH}/V_{SV})^2$$



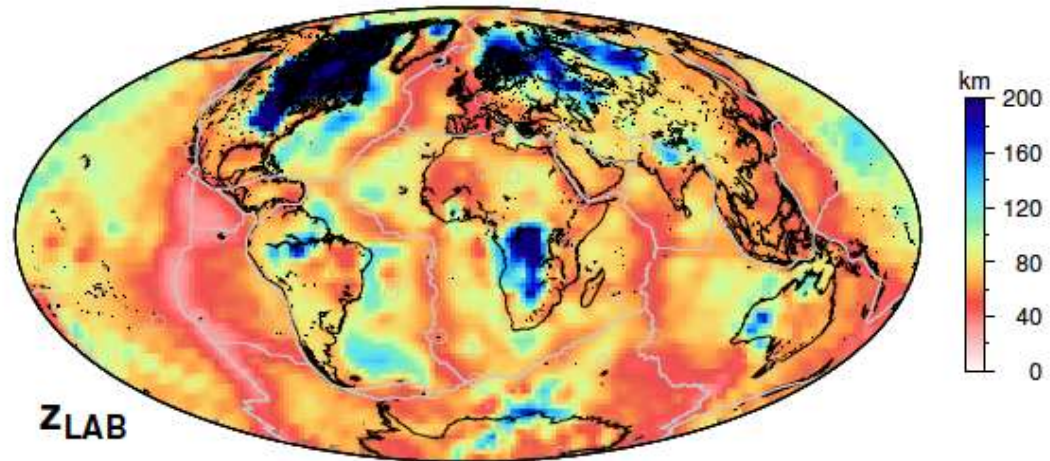
LAB from the change of orientation of azimuthal anisotropy Ψ_G



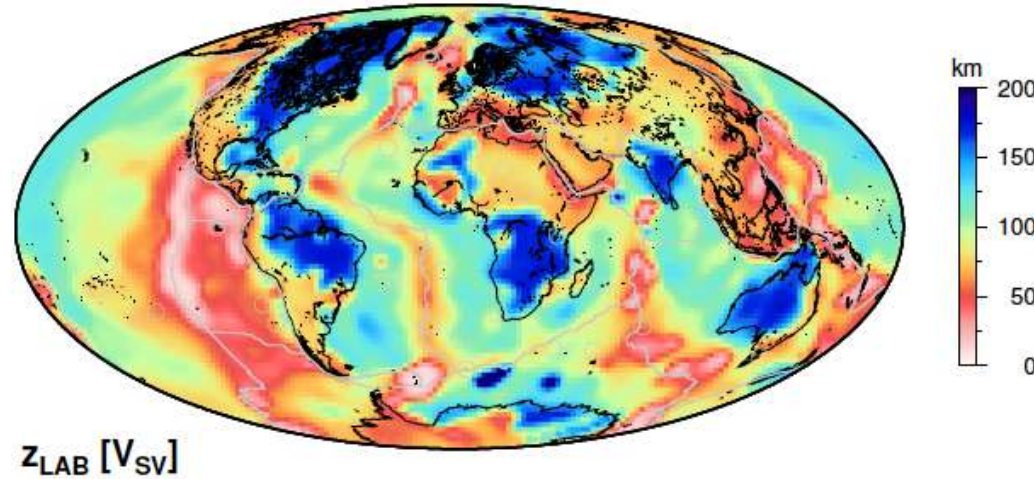
Correlation between plate motion given by NUVEL-1 and the orientation Ψ_G of fast axis of SV-wave azimuthal anisotropy G



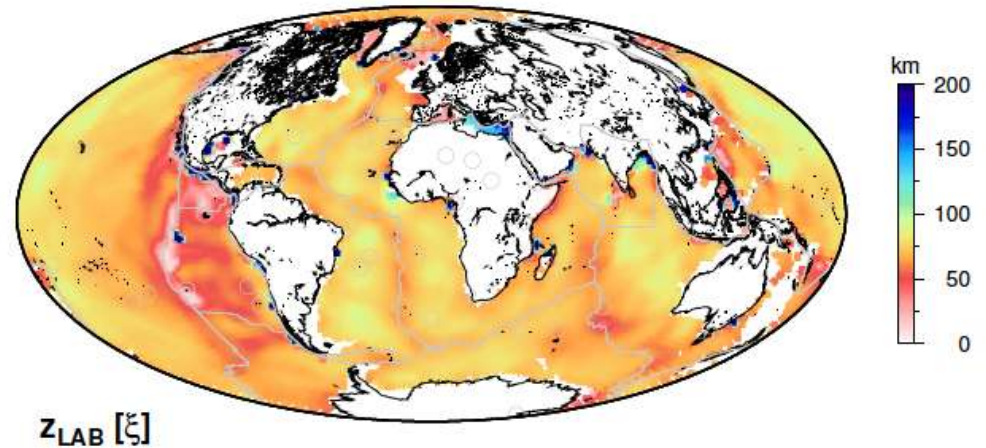
Vs Statistical MC Inversion



Vsv proxy (1st order
Perturbation Theory)

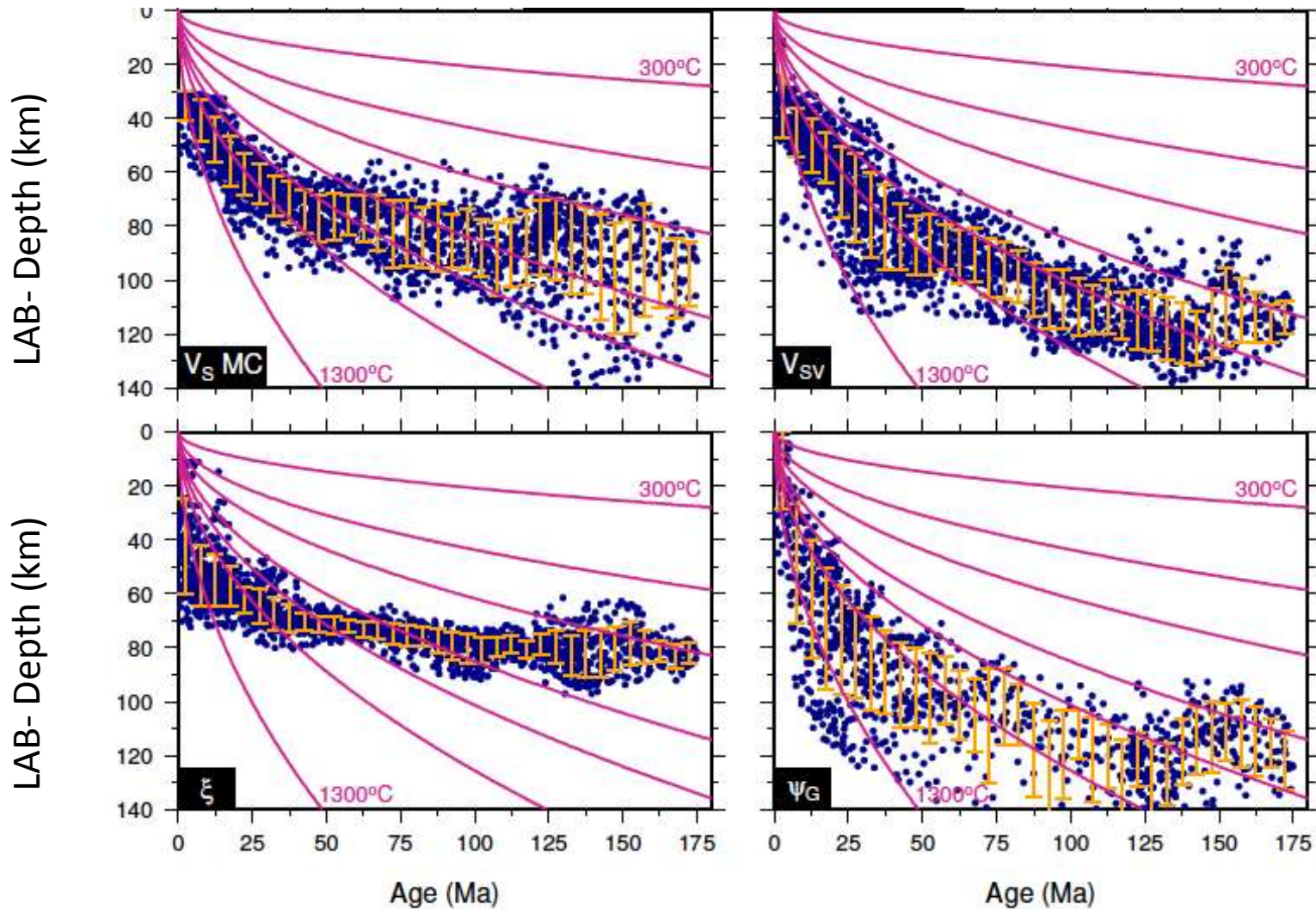


ξ proxy (1st order
Perturbation Theory)



Age Variation of LAB depth in oceanic regions

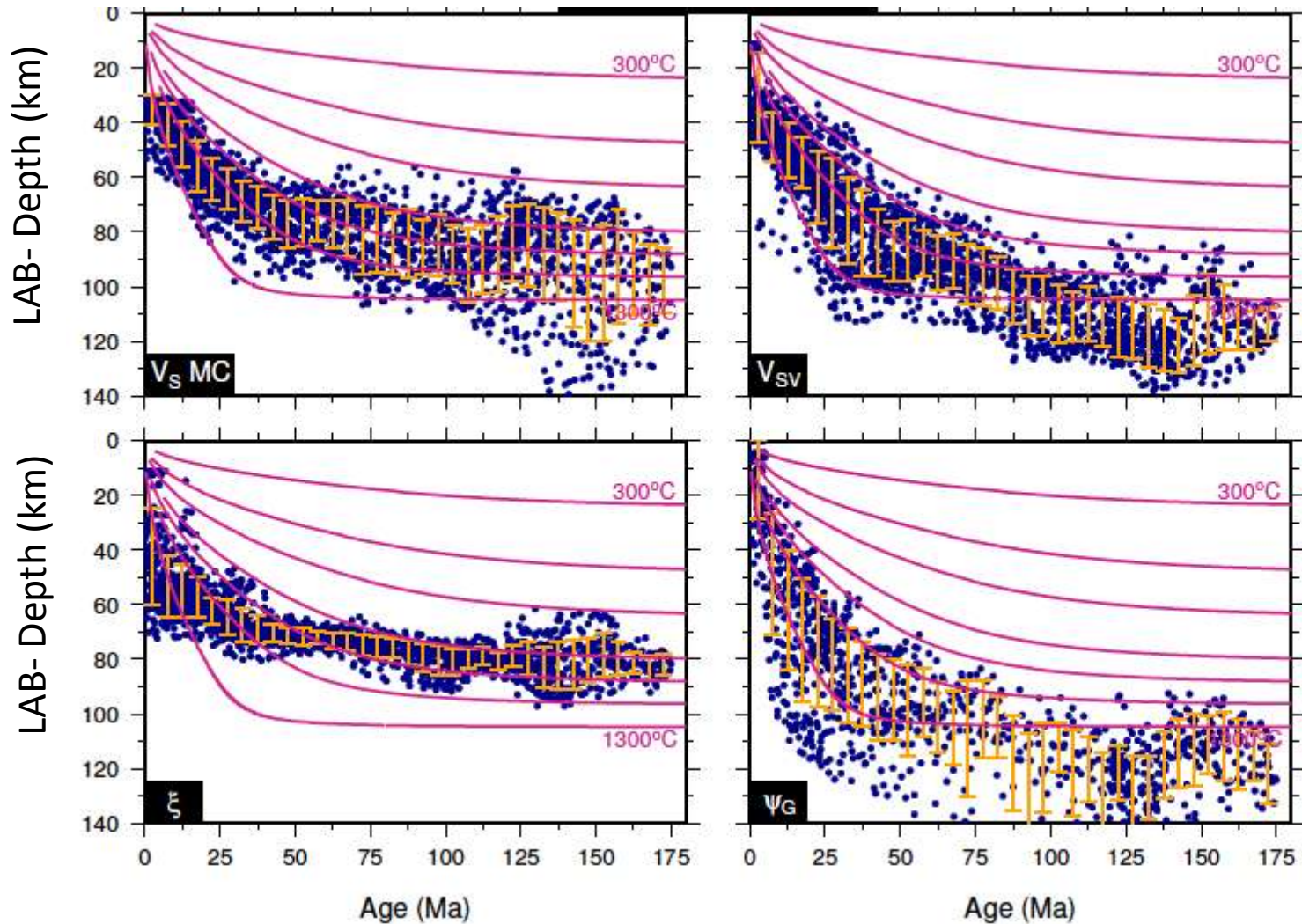
Compared with Half Space Cooling model



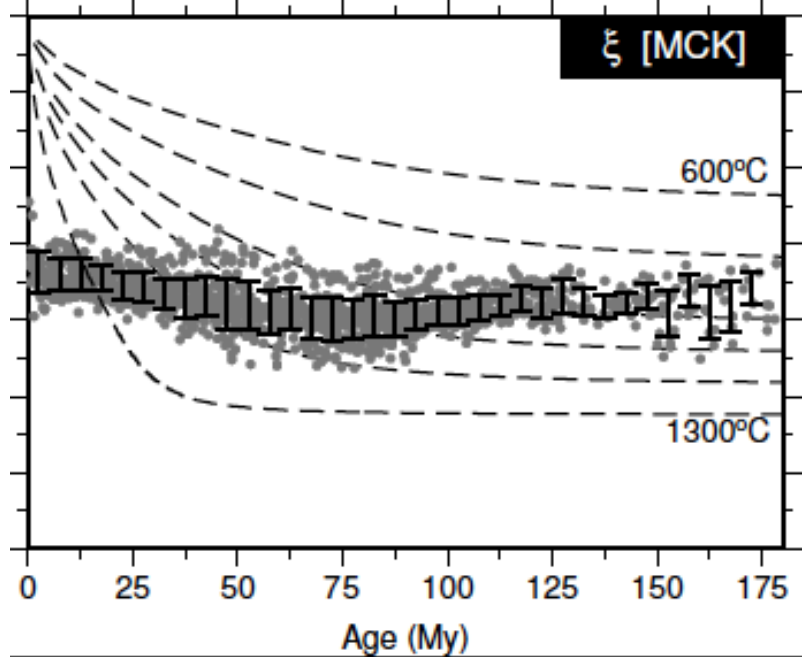
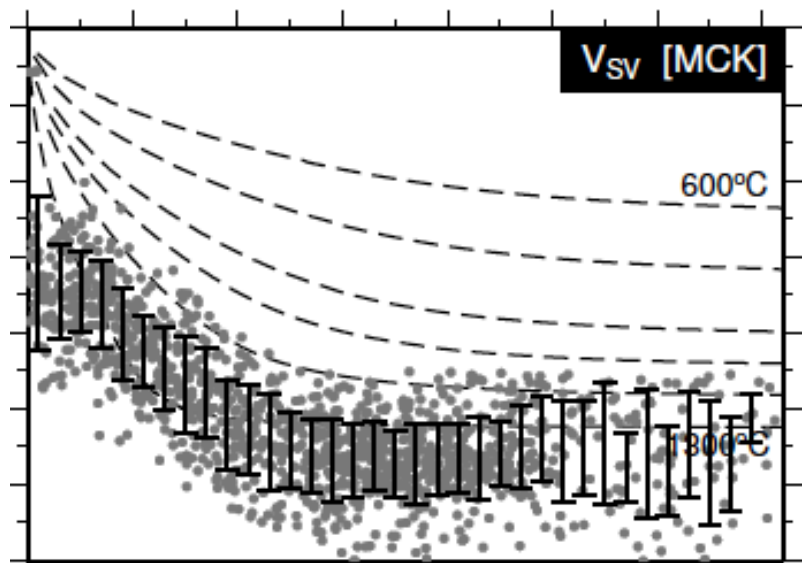
Age Variation of LAB depth in oceanic regions

Compared with plate model (McKenzie et al., 2005)

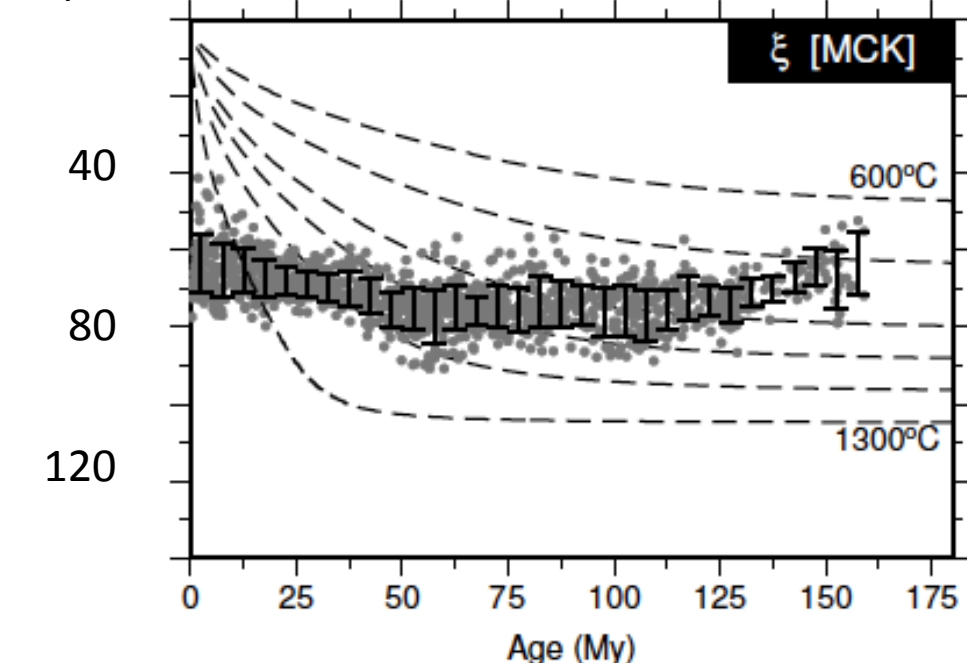
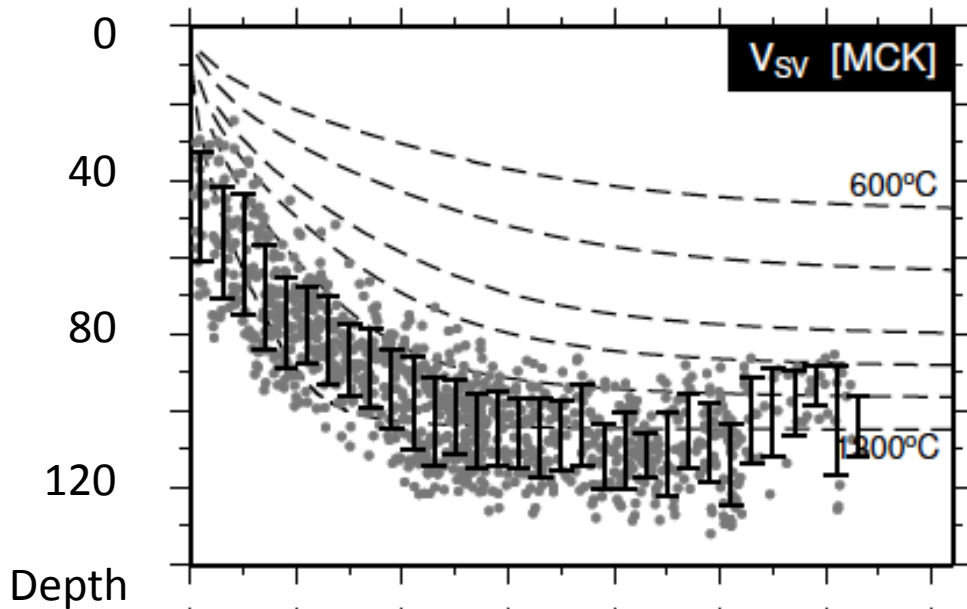
Pacific plate



Atlantic Ocean

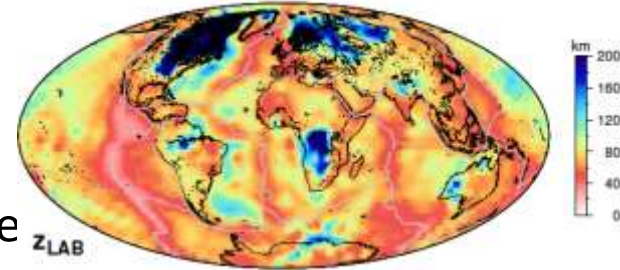


Indian Ocean

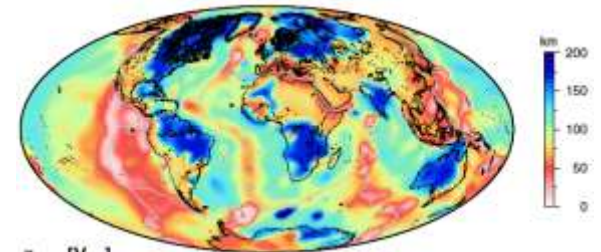


First Conclusions

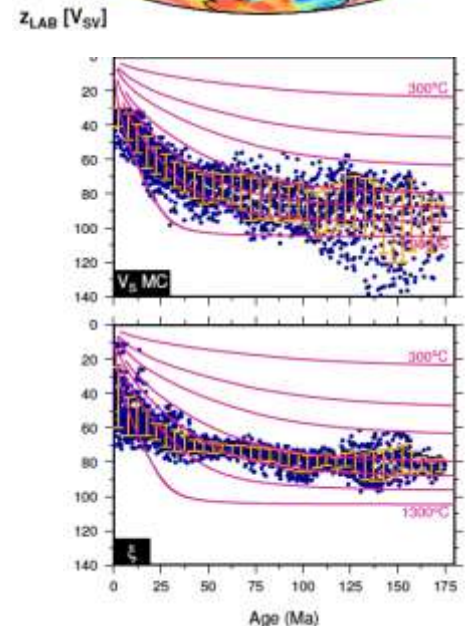
-LAB topography derived from surface wave data with 2 different inversion techniques (Monte-Carlo, 1st order perturbation theory) and for different proxies (S-wave velocity, radial anisotropy, azimuthal anisotropy)



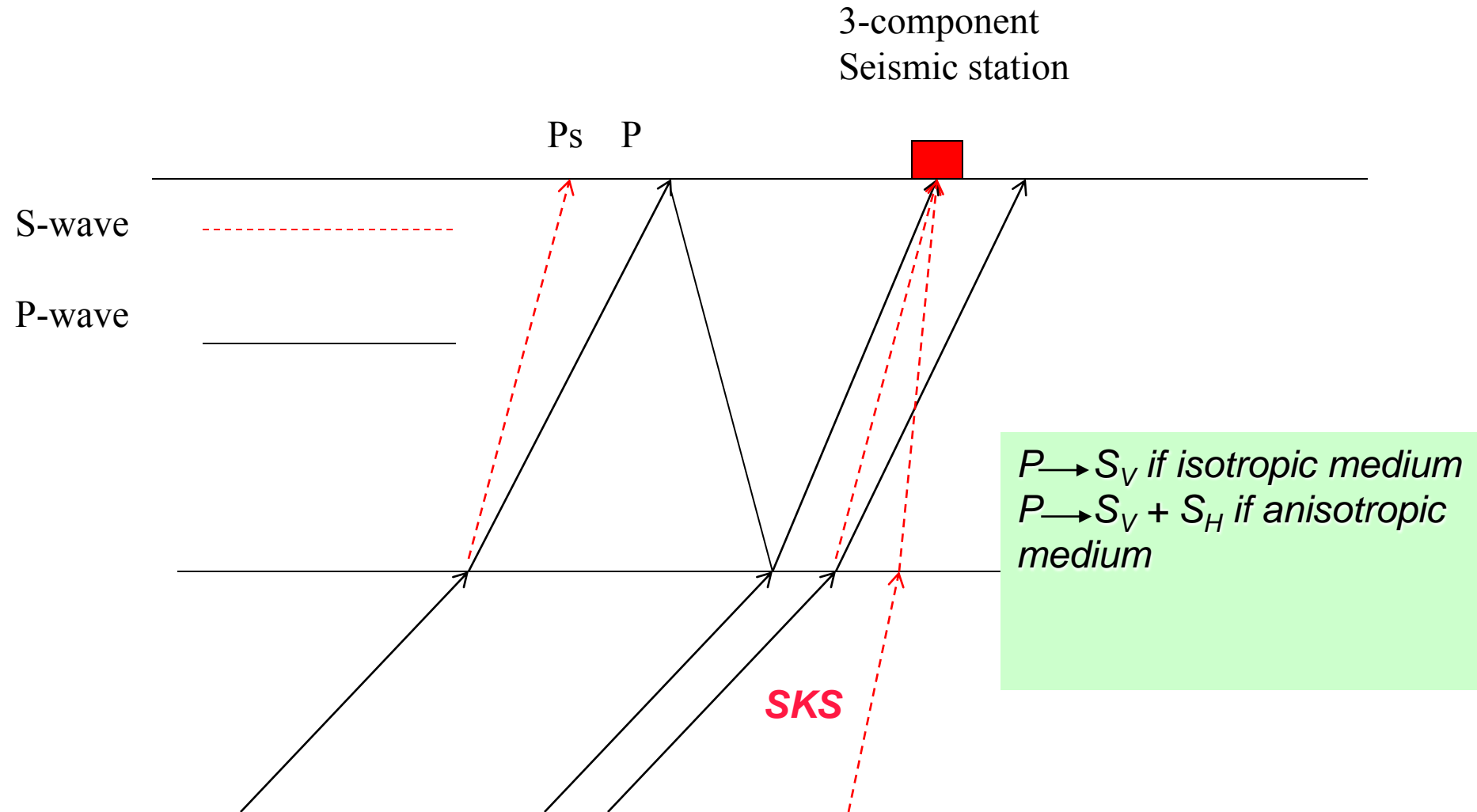
-Lateral variations of LAB (except from ξ) are similar but not their absolute values.



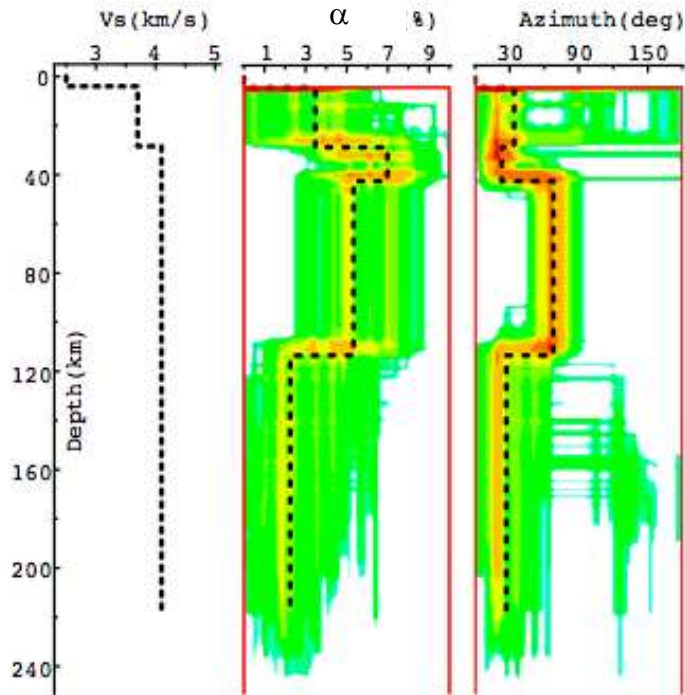
- For oceans, half-space cooling model does not work, plate model works slightly better, but the model of formation of lithosphere should be revisited in view of results from radial and azimuthal anisotropies.



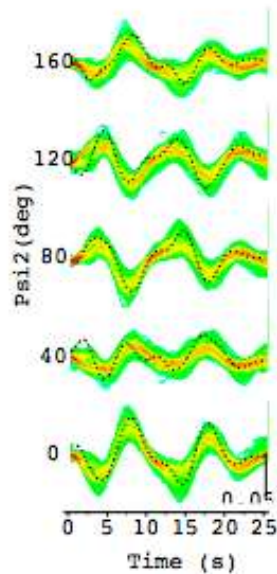
Simultaneous inversion of SKS and receiver functions: AFAR (Horn of Africa)



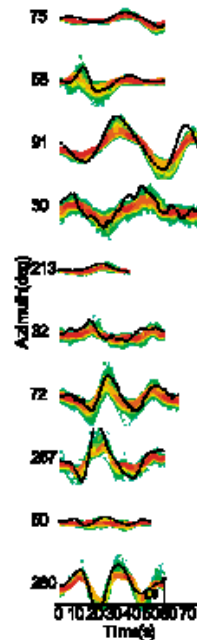
Geoscope ATD Station (Djibouti)



RF



SKS



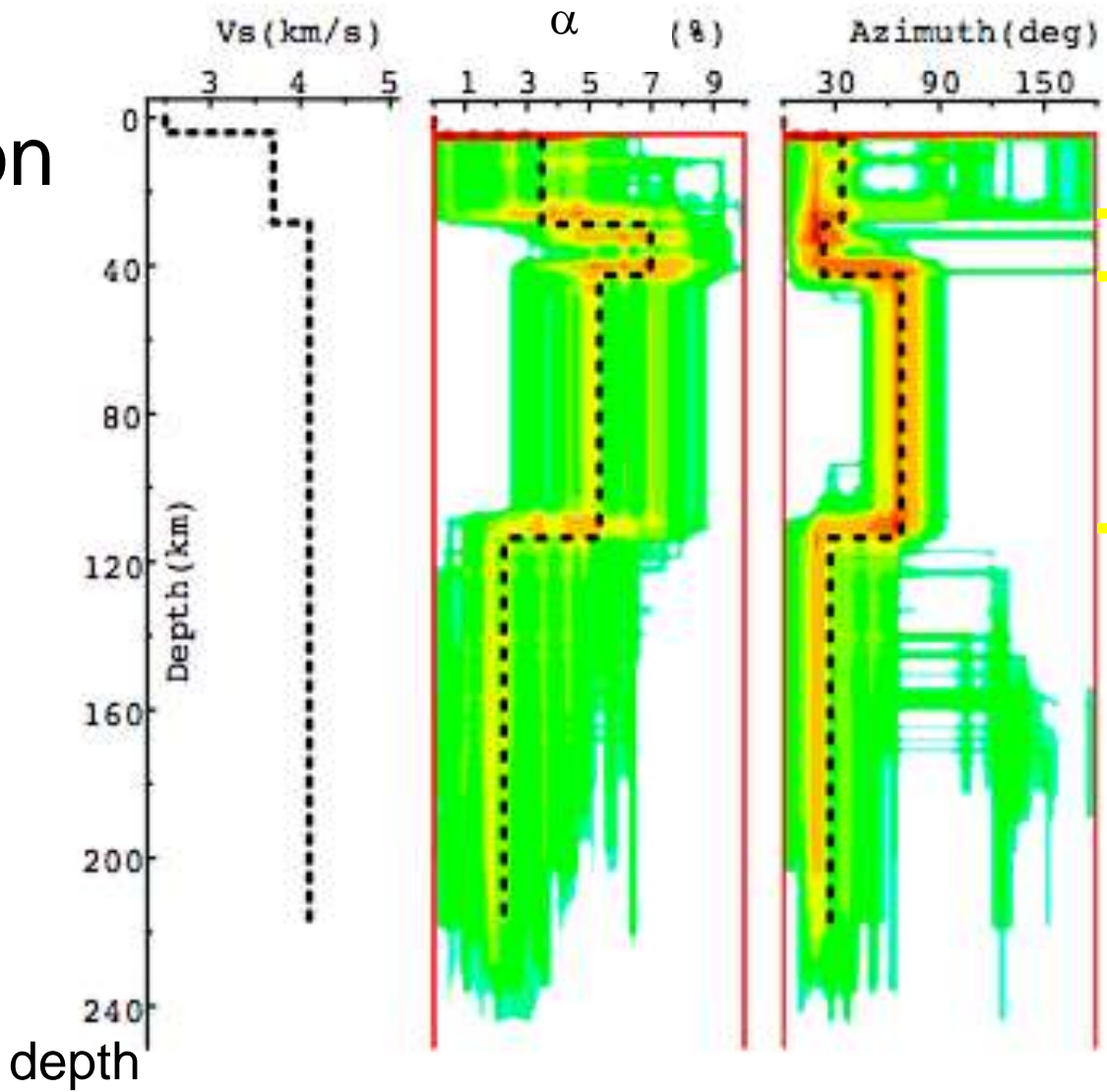
Receiver functions (RF)
+
SKS

Good Azimuthal Coverage

Obrebski et al., 2010

Simultaneous inversion of SKS and receiver functions

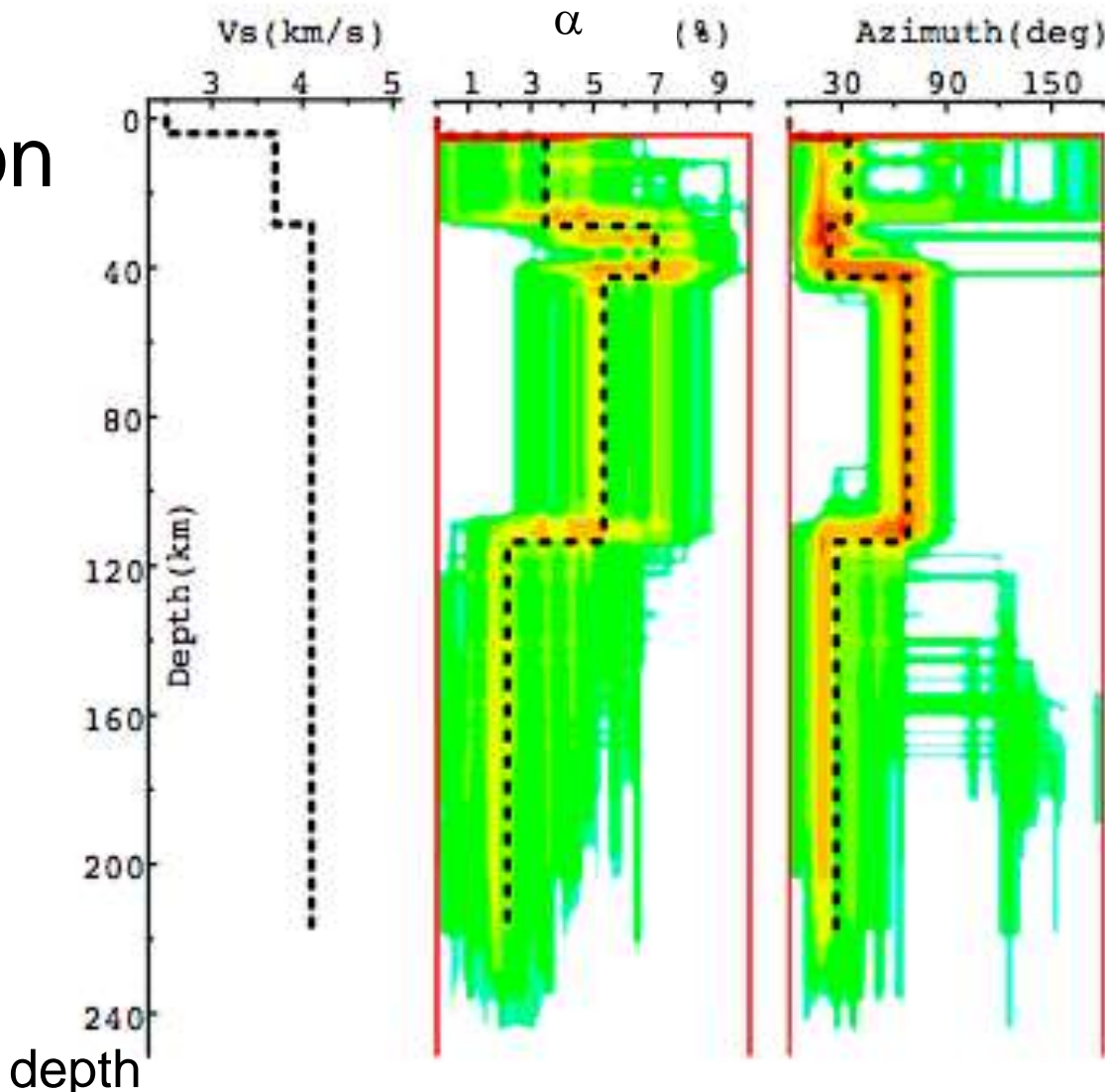
ATD
Station



Stratification

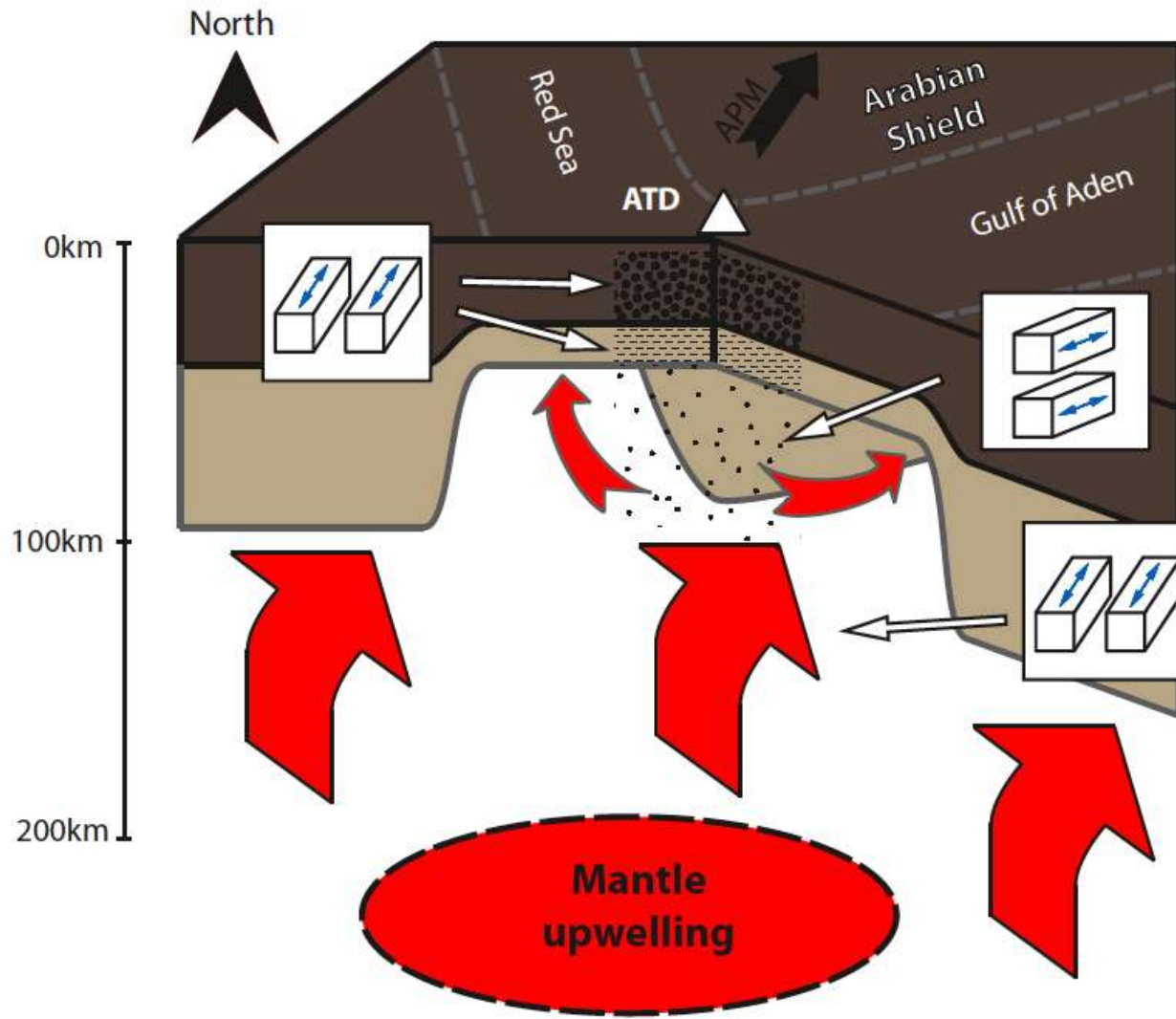
Simultaneous inversion of SKS and receiver functions

ATD
Station



Stratification

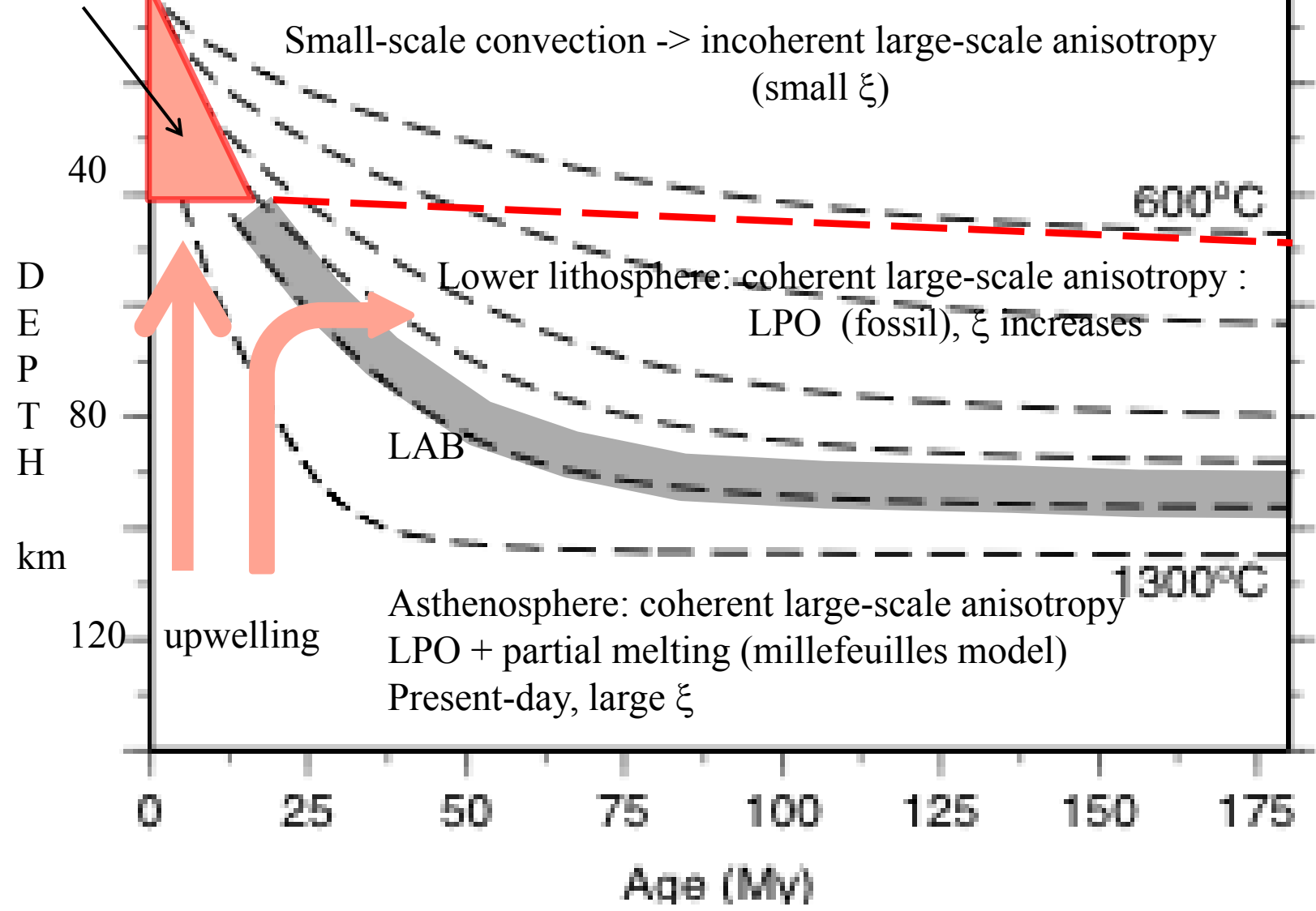
- Small anisotropy
- Coherent anisotropy: SPO
- Coherent anisotropy: LPO



Tentative tectonic model to explain the stratification of anisotropy around Afar.

Mixing of different processes in different layers

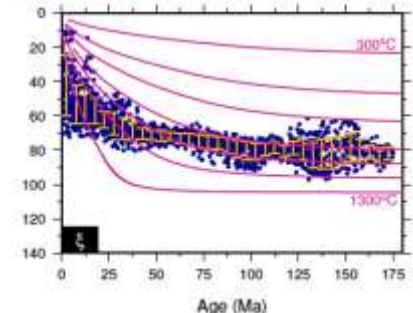
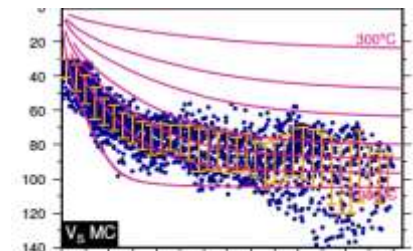
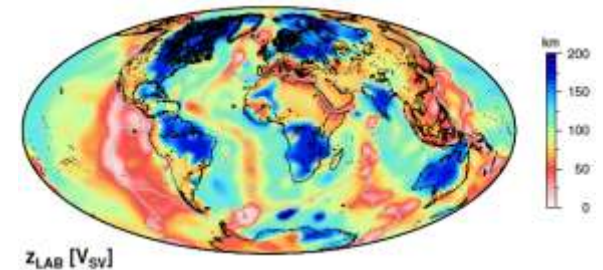
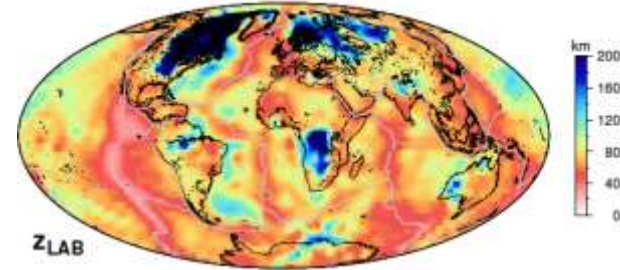
Partial melting



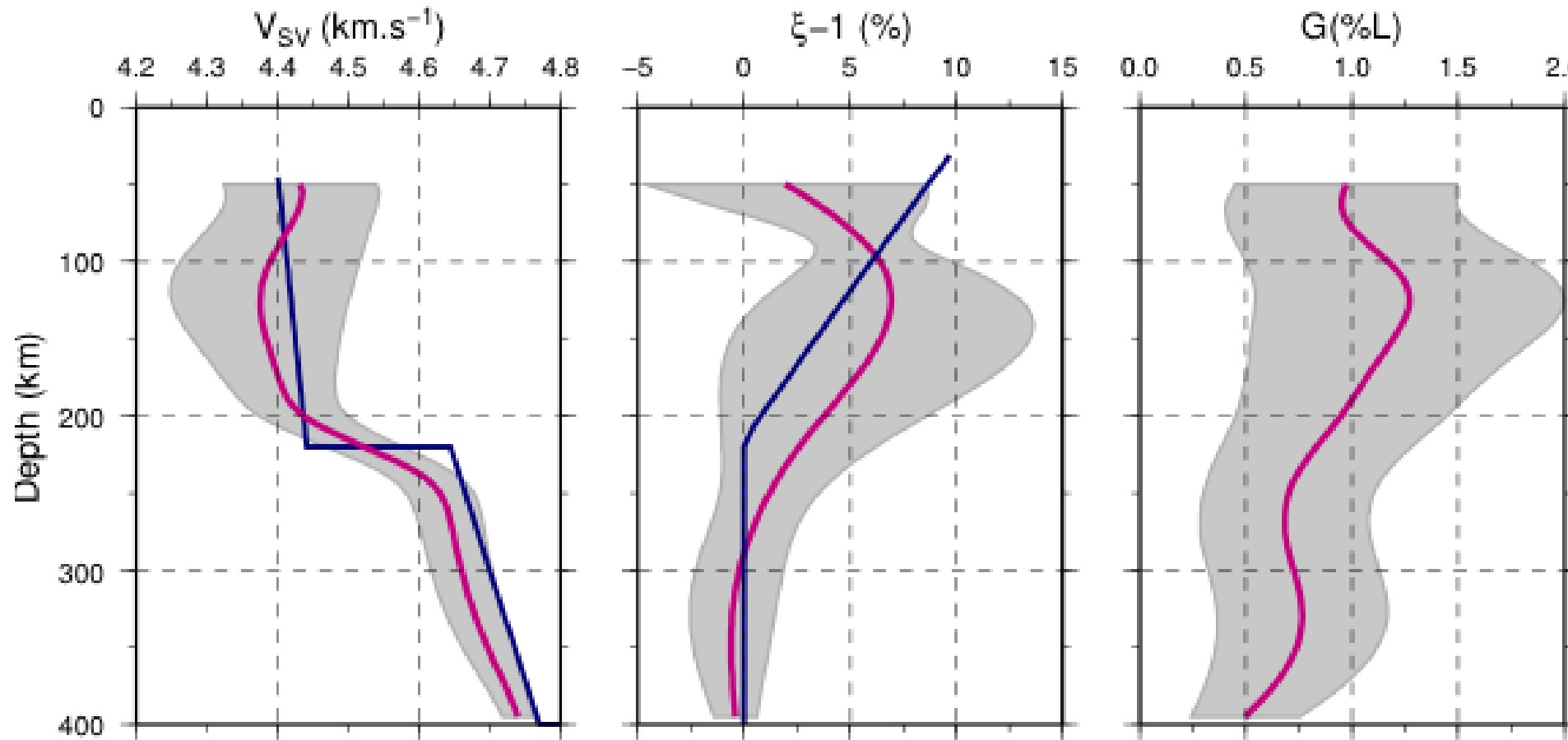
MLB: Mid-Lithospheric Boundary

Conclusions

- LAB topography derived from surface wave data with 2 different inversion techniques (Monte-Carlo, 1st order perturbation theory) and for different proxies (S-wave velocity, radial anisotropy, azimuthal anisotropy).
- Lateral variations of LAB (except from ξ) are similar but not their absolute values.
- For oceans, half-space cooling model does not work, plate model works slightly better, but the model of formation of lithosphere should be revisited in view of results from radial and azimuthal anisotropies.
- For oceans **mid-lithospheric discontinuity** derived from ξ .
- LAB in continents is more difficult to investigate (need to jointly use surface wave and SKS data).



Average seismic parameters below oceans

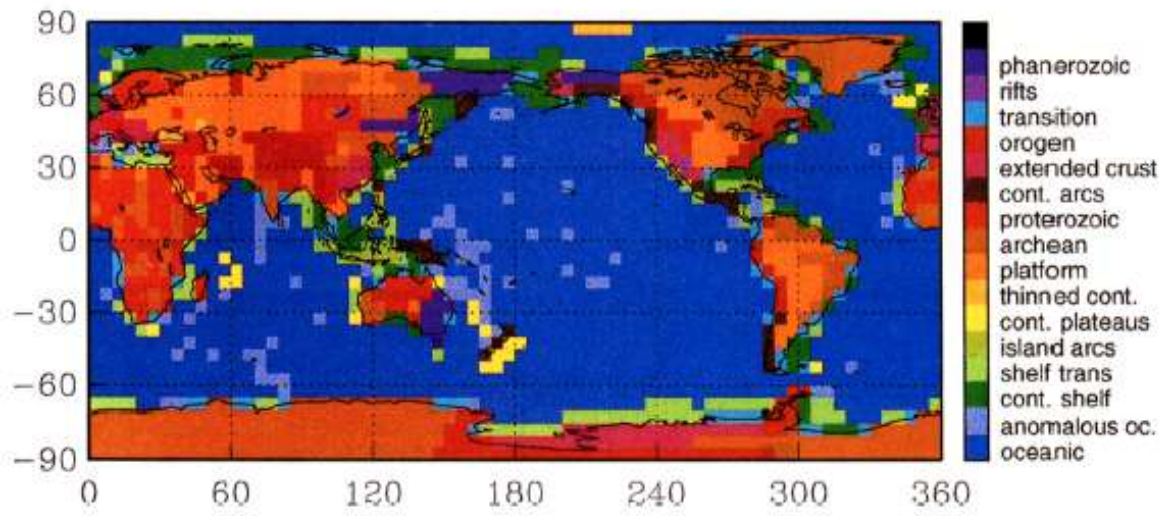


Crustal model:

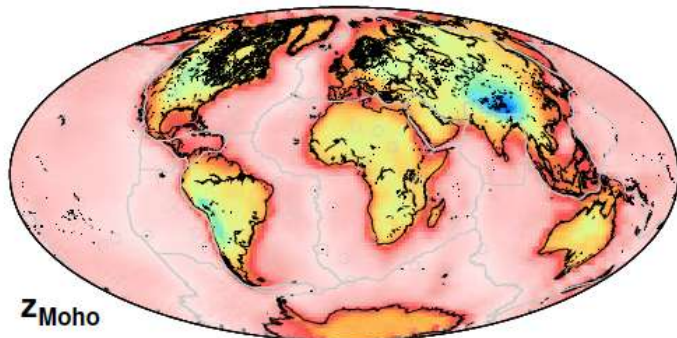
Improvement of the crust2.0 Model (Bassin et al., 2000)

Joint Monte-Carlo inversion of Rayleigh, Love phase, group velocity dispersion curves:

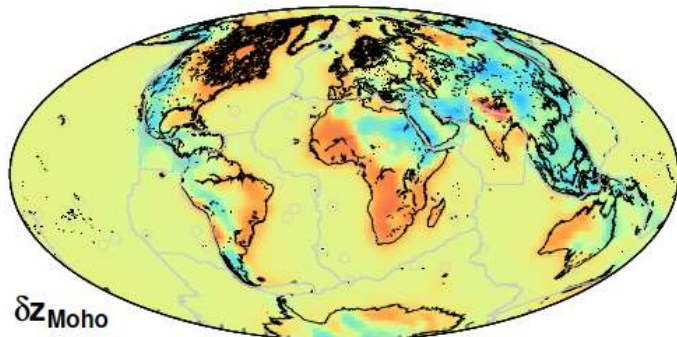
$$d=[C_R \ C_L \ U_R \ U_L]$$



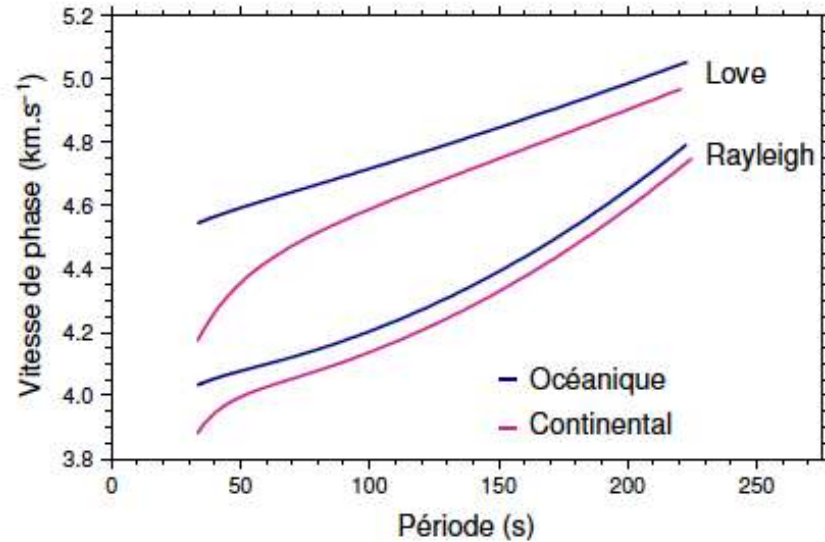
Mooney et al., 1998; Bassin et al., 2000



Z_{Moho}



δZ_{Moho}

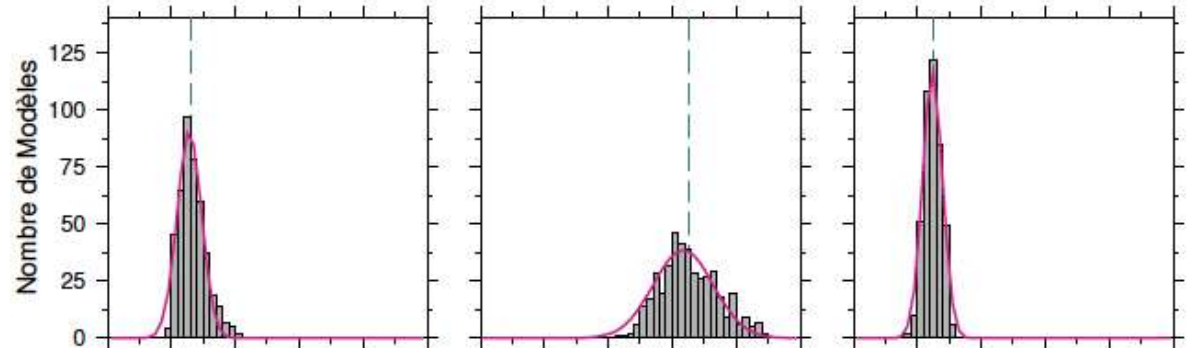
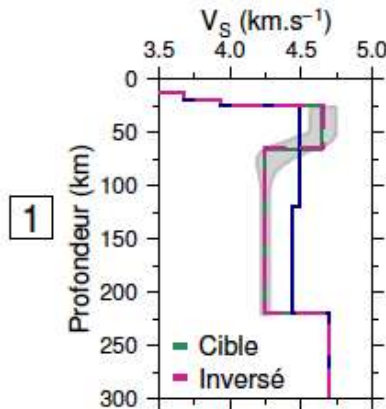


Sensitivity of surface waves to the LAB

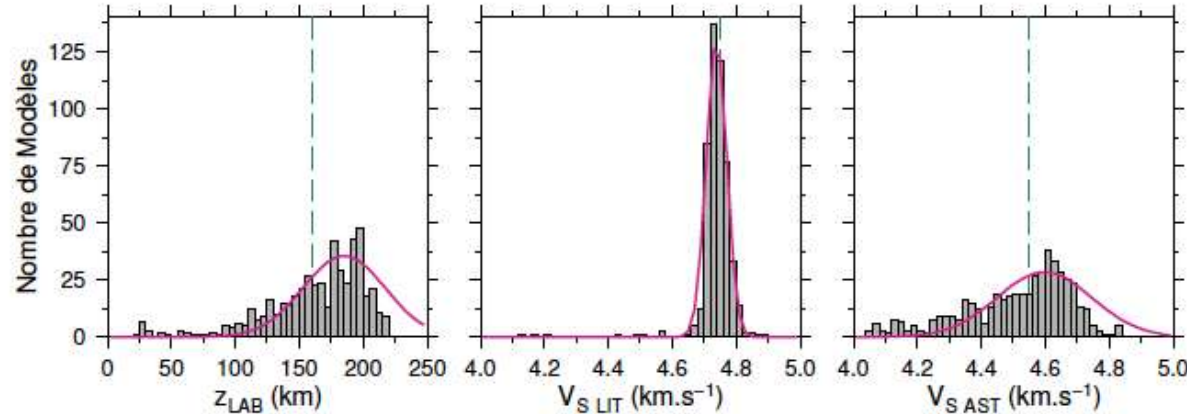
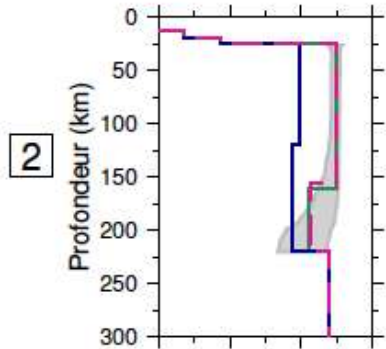
Red: starting model,
Grey Monte-Carlo Inversion

Grey Monte-Carlo Inversion

OCEAN



CONTINENT



Méthode du rejet

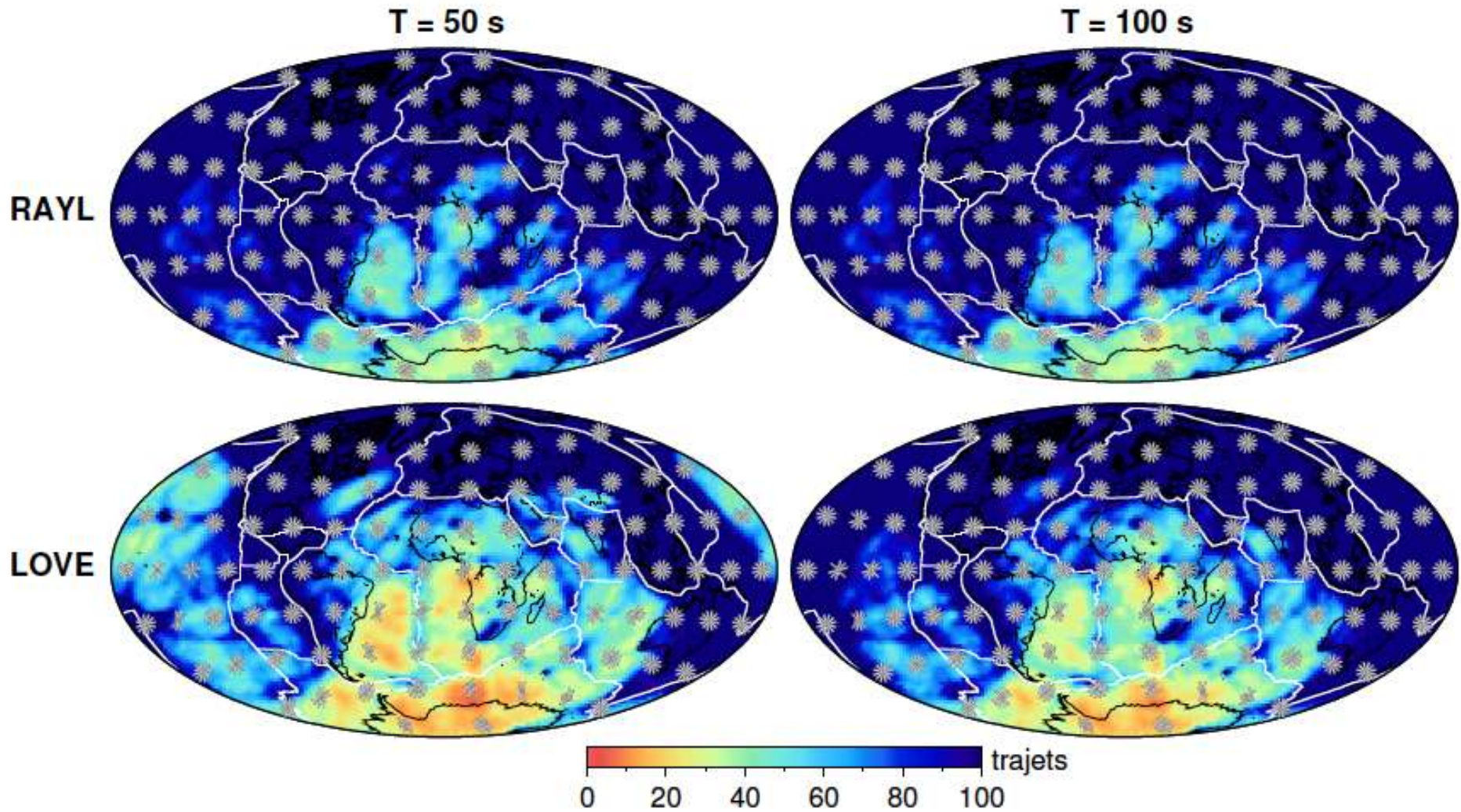
Paramètres : 2 V_S , 1 δZ

1 Océanique : $\delta Z_{LAB} \sim 5$ km

2 Continental : $\delta Z_{LAB} \sim 35$ km

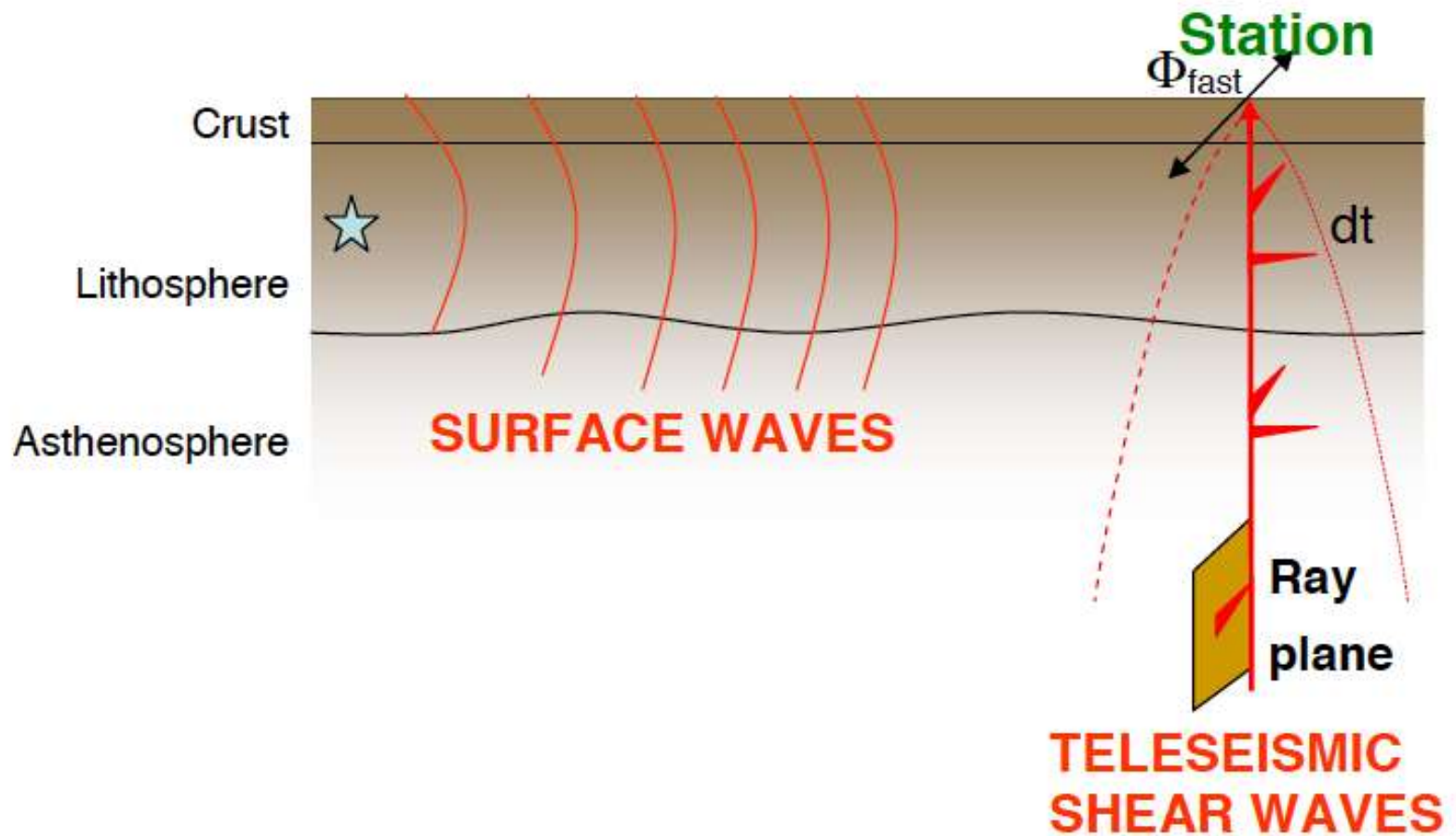
Path and azimuthal coverages of the merged dataset

Rayleigh, Love: C_R , C_L , U_R , U_L



Continental LAB: more complex

Joint anisotropic inversion of body wave and surface wave data



Wuestefeld et al., 2009

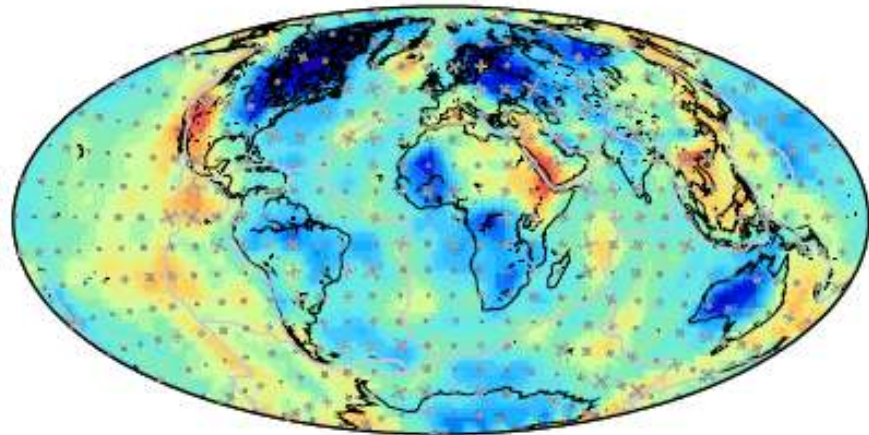
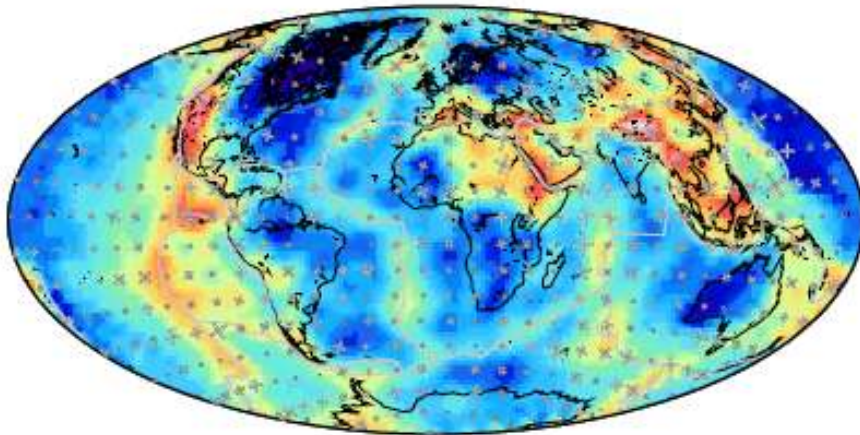
For SKS and S.W. Montagner et al., 2000

Cartes des vitesses de phase $0\psi+4\psi$

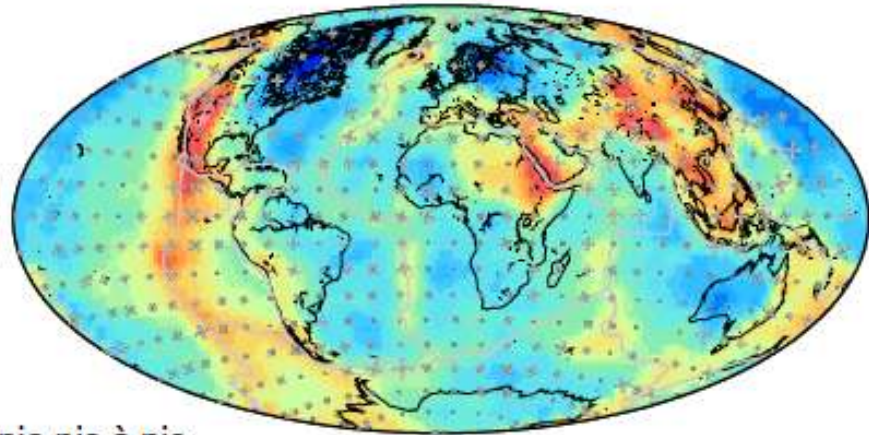
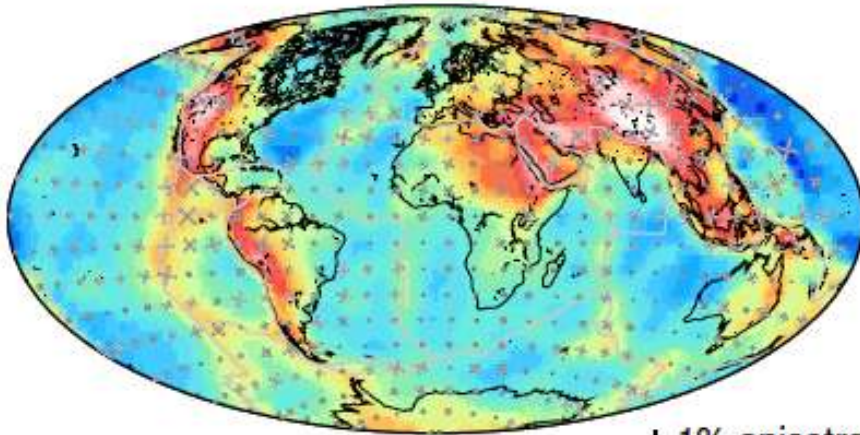
T = 50 s

T = 100 s

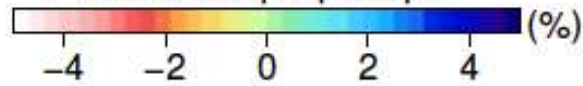
RAYL



LOVE



1% anisotropie pic à pic

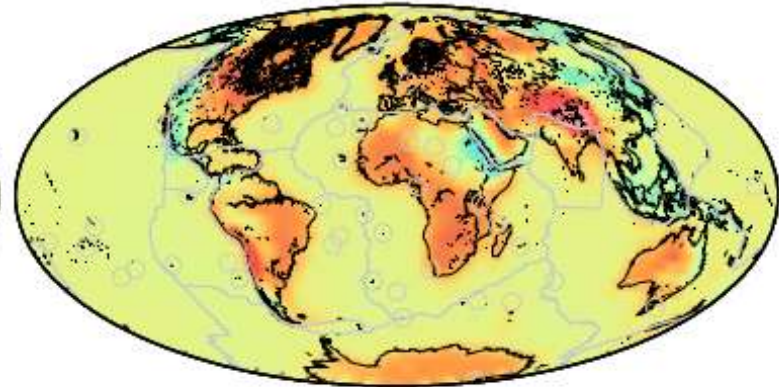
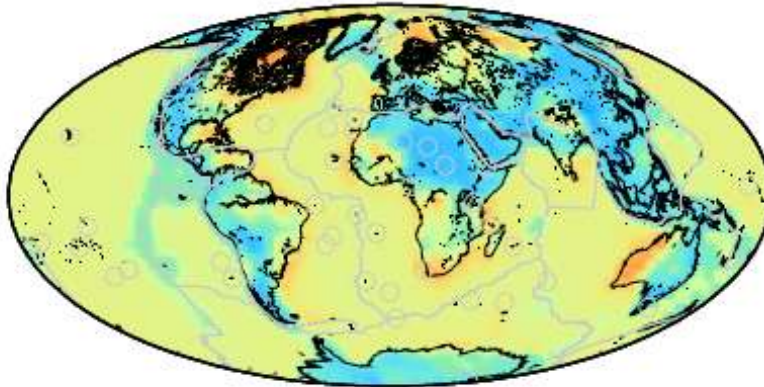


Inversion des données séparées

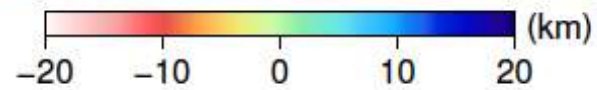
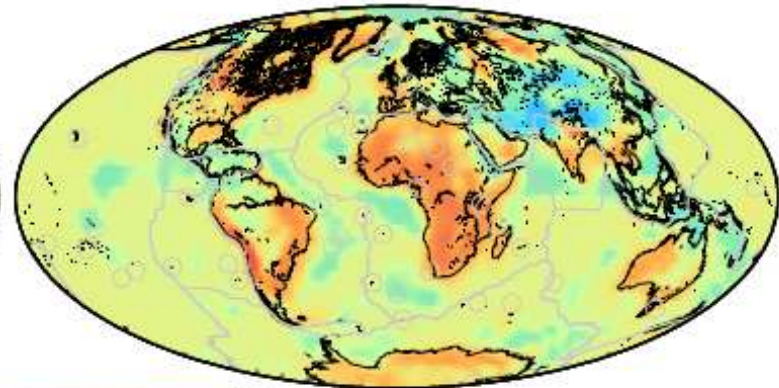
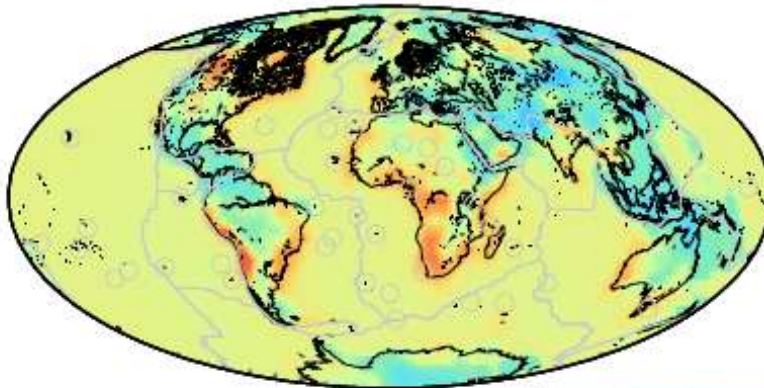
RAYL

LOVE

PHASE



GROUPE



Inversion Monte-Carlo

Paramètres : 3 V_S , 1 δZ .

Données : C_R , C_L , U_R , U_L [20-50s].

Différentes méthodes de Monte-Carlo.

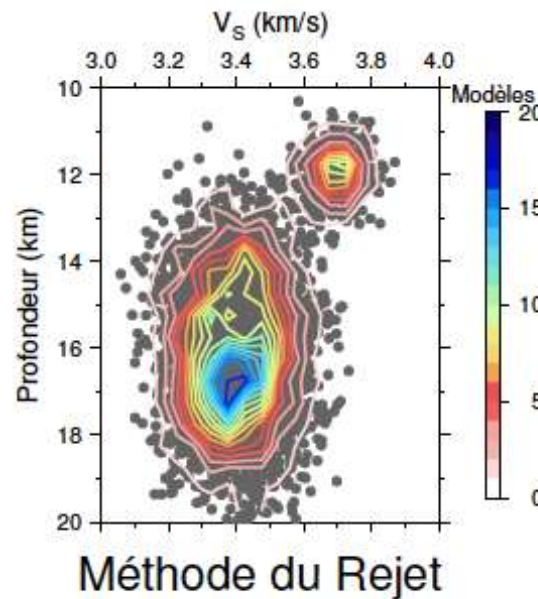
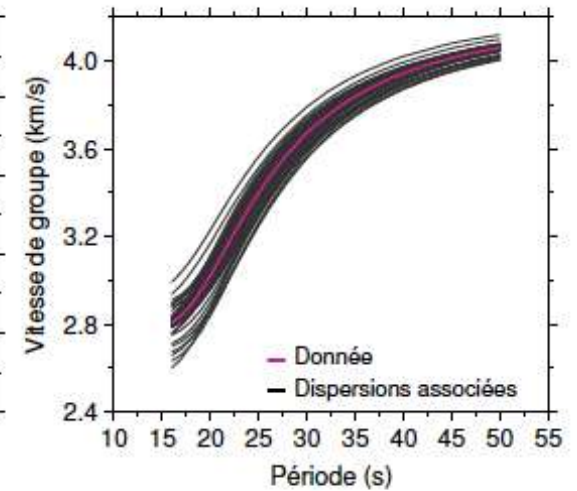
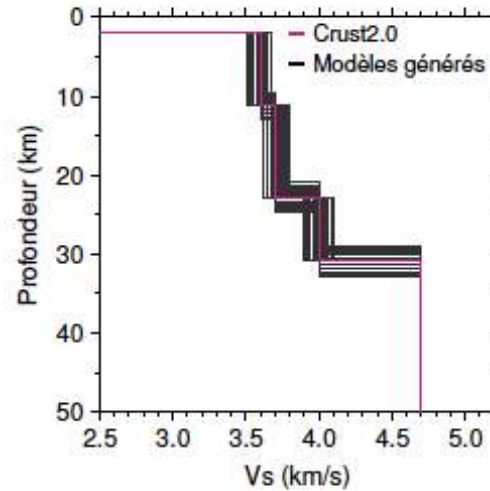
Fonction coût :

$$s_i = \sum_k^n \frac{(d_k^i - d_k)^2}{\sigma_k}$$

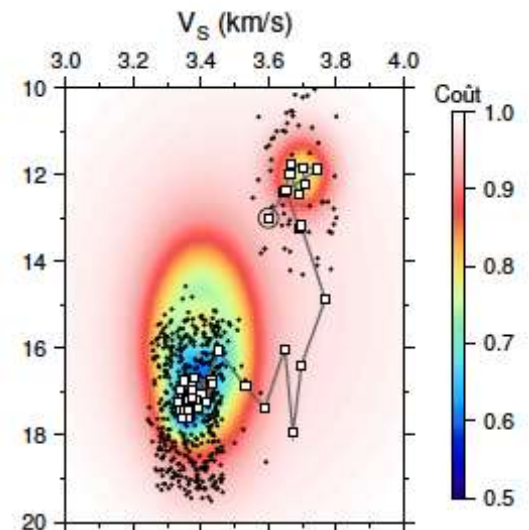
Probabilité d'acceptation :

$$P_i = \begin{cases} \exp\left(\frac{-(s_i - s_j)}{T_i}\right) & s_i \geq s_j \\ 1 & \text{pour } s_i < s_j \end{cases}$$

Routine de calcul de dispersion très rapide (*Herrmann, 1996*).



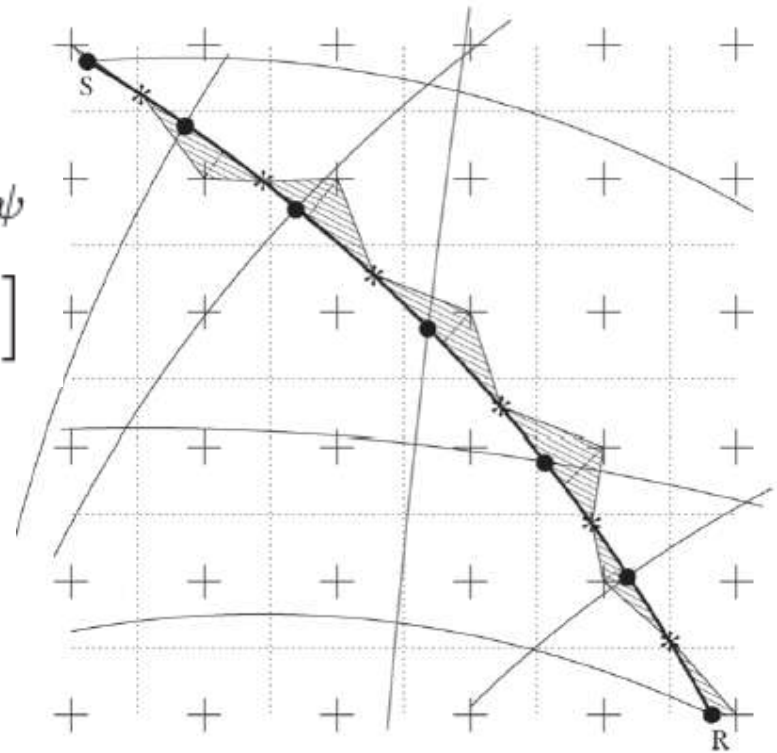
Méthode du Rejet



Recuit Simulé

$$\frac{\Delta}{C(T, \text{trajet})} = \int_S^R \frac{ds}{C(T, \theta, \phi)}$$

$$C(T, \psi) = C_i(T) \left[1 + \alpha_1(T) \cos 2\psi + \alpha_2(T) \sin 2\psi + \alpha_3(T) \cos 4\psi + \alpha_4(T) \sin 4\psi \right]$$



Beucler, 2002

Inversion en profondeur

Paramétrisation complètement anisotrope du manteau supérieur.

13 paramètres : $[\rho, A, L, \xi, \phi, \eta, B_C, B_S, E_C, E_S, G_C, G_S, H_C, H_S]$.

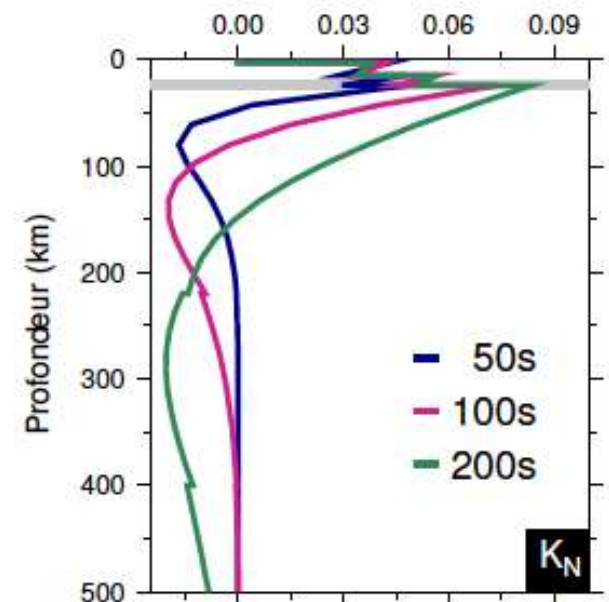
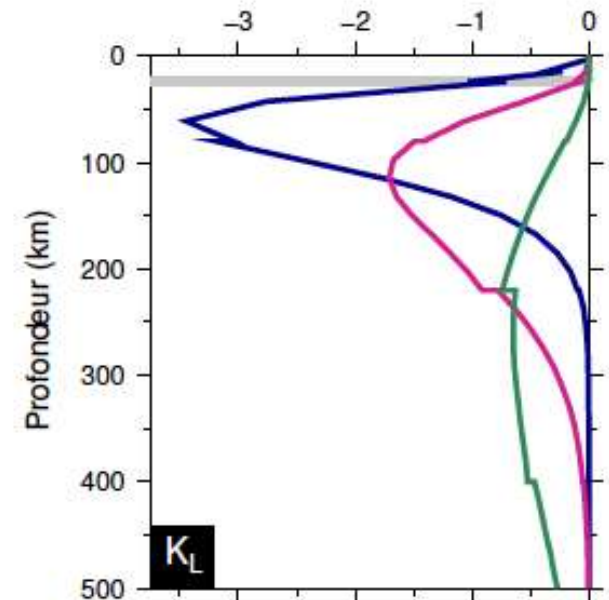
Données : $C_R, \alpha_R^*, C_L, \alpha_L^*$ [35-300s].

Inversion moindres carrés, théorie de la perturbation au 1^{er} ordre.

$$\begin{aligned} \delta C_R|_{k,\psi} = \int_{\Omega} & \left[\frac{\partial C_R}{\partial A} \Big|_k (\delta A + B_C \cos 2\psi + B_S \sin 2\psi + E_C \cos 4\psi + E_S \sin 4\psi) \right. \\ & + \frac{\partial C_R}{\partial C} \Big|_k \delta C + \frac{\partial C_R}{\partial F} \Big|_k (\delta F + H_C \cos 2\psi + H_S \sin 2\psi) \\ & \left. + \frac{\partial C_R}{\partial L} \Big|_k (\delta L + G_C \cos 2\psi + G_S \sin 2\psi) \right] d_{\Omega} / \Delta_{\Omega} \\ \delta C_L|_{k,\psi} = \int_{\Omega} & \left[\frac{\partial C_L}{\partial L} \Big|_k (\delta L - G_C \cos 2\psi - G_S \sin 2\psi) \right. \\ & \left. + \frac{\partial C_L}{\partial N} \Big|_k (\delta N - E_C \cos 4\psi - E_S \sin 4\psi) \right] d_{\Omega} / \Delta_{\Omega} \end{aligned}$$

(code modifié de *Montagner, 1986*)

Paramètres résolus : V_{SV}, ξ, G_C, G_S .

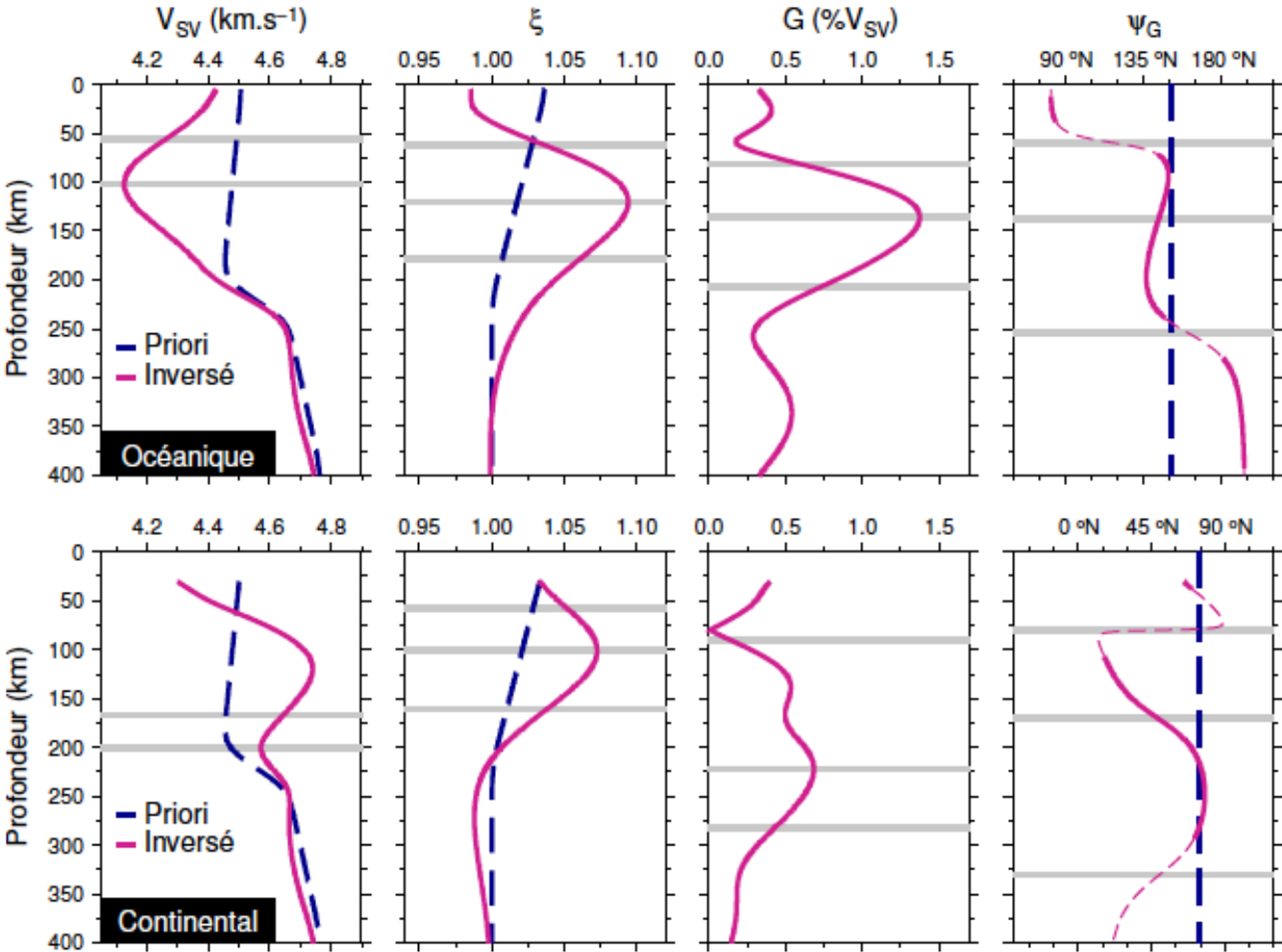


Paramètres du modèle tomographique

Paramètres résolus :
 V_{SV} , ξ , G_c , G_s .

Profil océanique
($\lambda = 35^\circ$, $\phi = -35^\circ$).

Profil continental
($\lambda = 63^\circ$, $\phi = -96^\circ$).



CRUSTAL MODEL

Joint M.C. inversion

$$d = [C_R \ C_L \ U_R \ U_L]$$

~25% variance reduction
wrt *a priori* Crust2.0

δz_{Moho} : difference between
Our model and crust2.0

